



ADDIS ABABA UNIVERSITY
SCHOOL OF GRADUATE STUDIES
FACULTY OF TECHNOLOGY

ANALYSIS OF ELECTRONIC ATTACK UNDER UAV
PLATFORM JAMMING

**A thesis submitted to the School of Graduate Studies of Addis Ababa
University in partial fulfillment for the Degree of Master of Science in
Communication Engineering**

By
Ashagrie Getnet

Advisor
Prof. DP. Roy

ADDIS ABABA

2008



ADDIS ABABA UNIVERSITY
SCHOOL OF GRADUATE STUDIES
FACULTY OF TECHNOLOGY

ANALYSIS OF ELECTRONIC ATTACK UNDER UAV
PLATFORM JAMMING

BY

Ashagrie Getnet

Approval by Board of Examiners

_____	_____
Chairman, Department of Electrical and Computer Engineering	Signature
_____	_____
Advisor	Signature
_____	_____
External Examiner	Signature
_____	_____
Internal Examiner	Signature

ACKNOWLEDGMENTS

I would like to acknowledge the following for help, encouragement, and support during the preparation of this thesis. First, I thank God for giving me the endurance and perseverance to complete this work. I could not have completed this work without the continuous support of my advisor DP. Roy and my wife Dr. Alemenshe Woldeyes. Special thanks to the member of INSA (Information Network Security Agency): Gebremeske T/Mariam, Abebe Demessie and Ahemed Hameza who have largely been the driving force behind this work. I am very thankful to my friends: Misrak Menber, Tsegay Teklu, Fantaye Mekonnen, Muna Seifu and Gezahgn Geleta for their encourage, constructive comments, and supporting in pursuing this work.

TABLE OF CONTENT

PAGES

ACKNOWLEDGMENTS.....	i
ABSTRACT.....	ii
LIST OF FIGURE.....	iv
LIST OF TABLE.....	viii
LIST OF ACRONYMS.....	ix
CHAPTER 1 INTRODUCTION.....	1
1.1 Background of the problem.....	1
1.2 Objective of the thesis.....	2
1.3 Significant of the study.....	2
1.4 Methods.....	3
1.5 Organization of the Thesis.....	3
CHAPTER 2 THE EFFECT OF EW ON RADAR OPERATION.....	5
2.1 Overview.....	5
2.2 Radar.....	5
2.2.1 Radar Modulations and Parameter.....	6
2.2.2 Frequency Used for Radar.....	7
2.2.3 The Radar Cross Section of a Target.....	7
2.2.4 Types of Radars.....	8
2.2.5 Radar Performance.....	8
2.3 Electronic Attack.....	9
2.3.1 EA Effect on Radar.....	9
2.4. Jamming.....	10
2.4.1 Radar Jamming.....	11
2.5. UAV (Unmanned Aerial Vehicles).....	14
2.5.1 Categorizing Military Operations.....	15
2.5.2 Predator UAV.....	15
CHAPTER 3 UAV-PLATFORM JAMMER.....	17
3.1 Introduction.....	17
3.2 Simplified Block Diagram of a Jammer.....	17
3.3 Jammer Receiver and Transmitter.....	19
3.4 The Transmission Antenna.....	23
3.5 The Propagation Path to Target.....	23

3.6. Jammer Losses.....	24
3.6.1 Transmit and Receive Losses.....	24
3.6.2. Atmospheric Loss.....	24
3.6.3. Processing Losses.....	24
CHAPTER 4 JAMMER EQUATION.....	26
4.1 The Radar Equation.....	26
4.2 Jammer Equation.....	31
4.2.1 Self-Screening Jammers (Ssj).....	32
4.2.2 Noise Jamming.....	34
4.3 Repeater Jamming Equation.....	37
4.4. Range Reduction Factor.....	49
4.5 The Effect of Swerling, Loss and UAV length for jamming analysis...40	
4.6 Jammer Transmitting and Receiving Antennas.....	42
4.6.1 Directivity Gain and Beamwidth.....	42
4.6.2 Half-Wave Dipole.....	45
CHAPTER 5 DETECTION OF UAV-PLATFORM JAMMER.....	47
5.1 Properties of A Stationary Gaussian Noise.....	47
5.2 Detection Probability and False Alarm Probability.....	48
5.3 Pulse Integration.....	51
5.3.1 Coherent Integration.....	51
5.3.2 Non-Coherent Integration.....	52
5.4 Improvement Factor and Integration Loss.....	54
5.5 Detection of Fluctuating Targets.....	56
5.6 Threshold Selection.....	57
5.7 Probability of Detection for Fluctuation Target.....	58
5.7.1 Marcum case; no Fluctuation.....	58
5.7.2. Swirling case I.....	60
5.7.3. Swirling case II.....	62
5.7.4 Swerling case III.....	64
5.4.8 Swerling case IV.....	65
CHAPTER 6 SIMULATION AND ANALYSIS OF JAMMER	69
CHAPTER 7 CONCLUSION AND FUTURE WORK	80

REFERENCE	82
APPENDIX A P-15 Radar Specification	85
APPENDIX B MATLAB CODE	86

LIST OF FIGURE

Figure Number	Pages
Figure 2.1 <i>Component of EW</i>	5
Figure 2.2 <i>Pulse repetition frequency</i>	6
Figure 2.3 <i>Radar-jamming geometry</i>	11
Figure 2.4 <i>Radar-jamming J/S factors</i>	12
Figure 2.5 <i>Stand-off and Stand-in jamming geometry</i>	12
Figure 2.6 <i>Self-protection jamming geometry</i>	13
Figure 2.7 <i>Noise jamming on a PPI display</i>	14
Figure 2.8 <i>Spot and Barrage jamming</i>	14
Figure 3.1 <i>Block diagram of UAV-Platform jammer</i>	18
Figure 4.1a <i>SNR versus detection range for three different values of radar peak power</i>	29
Figure 4.1b <i>SNR versus detection range for three different values of RCS ...</i>	30
Figure 4.2. <i>Pulse width versus required SNR for three different detection range values</i>	31
Fig. 4.3 <i>Power delivered to an antenna versus power radiated</i>	43
Fig. 4.4 <i>Polar and regular plots of normalized gain versus angle</i>	45
Fig. 4.5 <i>Beam solid angle and beamwidth of a highly directive antenna...</i>	45
Fig. 4.6 <i>Gain of half-wave dipole in dB units</i>	46
Figure 5.1 <i>Probability of detection versus SNR for several values of Pfa...</i>	50
Figure 5.2 <i>Simplified block diagram of a square law detector and non-coherent integration</i>	52
Figure 5.3. <i>Integration- Improvement factor (or equivalent number of pulses integrated) versus number of non-coherently integrated ...</i>	55
Figure 5.4. <i>Integration loss versus number of non-coherently integrated pulses</i>	56
Figure 5.5. <i>Threshold V_T versus np for several values of nfa</i>	58
Figure 5.6 <i>Probability of detection versus SNR and non- coherent $P_{fa}=10e-4$ integration</i>	59
Figure 5.7 <i>Probability of detection versus SNR single pulse $P_{fa}=10^{-4}$</i>	61

Figure 5.8 <i>Probability of detection versus SNR. Swerling I.....</i>	62
Figure 5.9 <i>Probability of detection versus SNR. Swerling II. $P_{fa} = 10^{-4}$...</i>	63
Figure 5.10 <i>Probability of detection versus SNR. Swerling III.....</i>	65
Figure 5.11 <i>Detection of Swerling IV Targets</i>	66
Figure 5.12 <i>Fluctuation loss versus probability of detection.....</i>	67
Figure 6.1 <i>Target and jammer echo signals... ..</i>	69
Figure 6.2 <i>Burn-through range versus jammer and radar peak powers corresponding to example used in generating Fig.6.1.....</i>	70
Figure 6.3 <i>$S/(J+N)$ versus detection range.....</i>	71
Figure 6.4 <i>Burn-through range versus ERP. $(S/(J+N)) = -34$ dB.....</i>	72
Figure 6.5 <i>Normalized range versus Jammer amplitude for SOJ.....</i>	72
Figure 6.6 <i>Range versus Jammer amplitude for SIJ.....</i>	73
Figure 6.7 <i>Range reduction factor versus radar operating wavelength.....</i>	74
Figure 6.8 <i>Range reduction factor versus radar to jammer range.....</i>	75
Figure 6.9 <i>Repeater jamming.....</i>	76
Figure 7.10 <i>Stand-off jamming effect using Swerling case.....</i>	77
Figure 6.11 <i>Stand-in jamming effect using Swerling case.....</i>	78

LIST OF TABLE

Table Number	Pages
Table 2.1 <i>UAV Technical Specification</i>	16
Table 3.1 <i>Jammer Loss</i>	25
Table 5.1 <i>Probability of detection for different Swerling case at SNR=12dB and fluctuation loss at Pd=0.9</i>	67

List of Acronyms

AOA	angle of arrival
BW	bandwidth
C₃	command, control and communication
CW	continuous wave
DDS	direct digital synthesizers
DF	directional finding
EA	electronic attack
ECM	electronic counter measure
EIRP	effective radiated power with respect to an isotropic radiator
EM	electromagnetic
EP	electronic protection
ES	electronic warfare support
ESM	electronic support measures
EW	electronic warfare
HPBW	half-power beam width
IW	information warfare
PA	pulse amplitude
PC	pulse compression
Pd	probability of detection
PDF	probability density function
Pfa	false alarm probability
PPI	plan position indicator
PRF	pulse repetition frequency
PW	pulse width
RCS	radar cross section

RPV	remotely piloted vehicle
SEAD	suppression of enemy air defense
SIGINT	Signals intelligence
SOJ	stand-off jammer
SIJ	stand-in jammer
SNR	signal- to- noise ration
UAV	unmanned air vehicle

Abstract

Ground base jammer cannot provide air space dominance for Ethiopia due to the massive highland complex of the country characterized by high rising mountains and dissected plateaus. In addition to this if high-flying systems and unsecured air space are piloted; it may be too dangerous in some situation to over fly certain areas. To overcome the above problem this thesis provides a good solution which is implementing a jammer on a UAV-platform. In this thesis, the Electronic Attack systems and the performance degradation of Surveillance Radar (P-15) due to UAV-platform jammer are described and analyzed. The jammer parameters were collected from simulation result as well as standards data. Using these parameters the effect of jamming on detection of targets is evaluated. The evaluation is performed by finding the change in radar SNR due to jamming and range reduction. The Predator-UAV type is the base system for this study much like the stand-off jammer. However, since the distance is closer to the radar, the EIRP jamming requirements are reduced. Stand-in jammer requires 6.3 watt at 50Km and stand- off jammer need 50 watt at 130Km from victim radar i.e. sufficient to jam P-15 Radar. For economical aspect stand-in jammer is much preferable for our country, since it provides 93% range reduction with a minimum amount of power.

CHAPTER 1

INTRODUCTION

1.1 Background of the problem

Electronic warfare (EW) is a military action whose objective is to control the *electromagnetic (EW)* spectrum. To accomplish this objective, both *offensive electronic attack (EA)* and defensive *electronic protection (EP)* action are required. Electronic attack involves Defense forces and platforms against hostile weapon, and C3 (command, control and communication) systems. In its traditional form (*self-protection*), EA consists of a warning receiver to warn of impending weapon attack (*attack warning*), expendable countermeasures, and a jamming system. The defensive protection aspects of attack warning and platform self-protection are strongly synergistic with the defensive measures and goals described in the Protection of Space Assets .More recent technology further expands the boundaries of electronic attack by engaging sophisticated, long-range target acquisition sensors— such as airborne and space-based surveillance/synthetic aperture radars, and the increasingly modern communications supporting all phases of the enemy attack or defense—thereby becoming a key, integral element of battle space dominance. In short, Electronic Warfare (EW) is vital to all types of military operation.

UAVs (Unmanned Aerial Vehicles) are also known as drones or remotely piloted vehicles . The Department of Defense defines a UAV as a powered aerial vehicle that does not carry a human operator, uses aerodynamic forces to provide lift, can fly autonomously or be piloted remotely, can be expendable or recoverable, UAV's have a vital role to play in the prosecution of EW campaigns. As a prominent, vital role in the new, “leveraged” concept of full-dimensional protection UAV's can contribute in all aspects of Electronic Warfare, from jamming and Suppression of Enemy Air Defense (SEAD) to Electronic Support Measures (ESM), and Signals Intelligence (SIGINT)[25].

UAVs are particularly important for surveillance when these operations could be conducted over days. In this sense, UAVs could relieve manned platforms of the need to maintain the high operational tempo for the extended periods that are the norm in modern military contingencies.

UAVs can be used to attack high-value, fixed ground targets in military operations. Once military commanders give the location, type of target, and desired weapons effects to the UAV, it would determine the proper way to attack the targets with a remote operator or some form of automation.

The following problems exist for Ethiopia military force relative to jamming:

- Ground base jammer can not provide air space dominance for Ethiopia due to a massive highland complex of mountains by nature;
- High altitude-flying systems and unsecured air space are to be piloted which may be too dangerous to fly over certain areas ;
- Tactical campaign plan almost change once the operation is on, in such situation ground base jammer is not flexible;
- Deploying ground base jammer need high cost.

1.2 Objective of the thesis

- The general objective of this thesis is to provide a good solution for the above problems, which is to facilitate the implementation of jammer on UAV-platform.
- The over all goal of the thesis is to get air superiority for our country; achieved by electronic attack (jamming).

Specific Objective

- To analyze detection range with UAV for the required jamming condition under the North-Ethiopian atmospheric condition.
- To design a specific jamming system for specific enemy threats, such as P-15 RADAR.

1.3 Significant of the Study

- The study is highly flexible to jam other than P-15 radar such as P-12, P-18, TPS 70 surveillance radars etc, with little modification.
- It helps for application of advanced techniques such as pulse compression.
- For practical design it provides a fundamental methodology to achieve a successful jamming.

1.4 Methods

Literature Review

In this thesis, the area concerning the existing problems of safeguarding air space and ground-space territory is studied. The mechanism that provides a solution for the real-time problems is collected. The role of UAV in ECM/EA techniques for various type of jamming technique, are collected to develop a design for specific jamming system.

Design

- Analysis of the problem
- Literature review
- Select a particular UAV platform for carrying jammer payload.
- Design a suitable jamming technique.
- Perform the required calculations and simulations.
- Present the results in a meaningful fashion.

Analysis

- Evaluate the performance of the UAV jammer subject to different hostile non-communication system or threats the so called P-15 radar system.
- Analyze the effectiveness of the jamming system taking in to consideration of various jamming parameter.

1.5 Organization of the thesis

The organization of this thesis is as follows:

Chapter 1: The first chapter describes the background and the objective of the thesis including the methodology of the study.

Chapter 2: The second chapter describes the most common concepts used in Electronic Warfare (EW) systems, some of the Electronic Warfare systems are Electronic attack (EA), Electronic protection(EP), Electronic Support (EP), Radar, and UAV. In addition to this it describe the effect of EW on Radar .This chapter select the particular radar and UAV type.

Chapter 3: Reviews jammer block diagram, including jammer transmitter, jammer receiver, and propagation path. The jammer loss is also analyzed. The concept of match-

filter is introduced.

- Chapter 4:** In this chapter, the jamming equations are developed, starting from the fundamental radar equation and then self-screen jamming, Stand-off and Stand-in jamming. The range reduction factor and Burn-through range are also derived.
- Chapter 5:** Is intended to provide an overview of the jammer probability of detection and related topics. Detection of fluctuating targets including Swerling I, II, III, and IV models are presented and analyzed. Coherent and non-coherent integration are also introduced.
- Chapter 6:** Using the above chapters the jammer parameters are found and the effect of this parameter is described, which includes jammer peak power versus radar peak power, S/J against the detection range. The effect of Swerling cases are also analysed using mat-lab simulation tools.
- Chapter 7:** Covers conclusion and future recommendation for this work.

CHAPTER 2

THE EFFECT OF EW ON RADAR OPERATION

2.1 Overview

EW is the art and science of denying enemy forces the use of the electromagnetic spectrum while preserving its use for friendly forces. EW is a significant force multiplier because it reduces friendly losses by defeating or reducing the effectiveness of enemy weapons.

As shown in Figure 2.1 EW is commonly divided into three subfields. Electronic support (ES) involves receiving enemy signals to identify and locate threat emitters and to help determine the enemy's force structure and deployment. Electronic attack (EA) involves measures taken to defeat enemy electronic assets. It includes jamming, chaff, directed energy weapons, and anti-radiation missiles. Electronic protection (EP) comprises countermeasures to enemy electronic attack. All of these concepts are applied at radar, communication, infrared, and laser operating systems [8, 25].

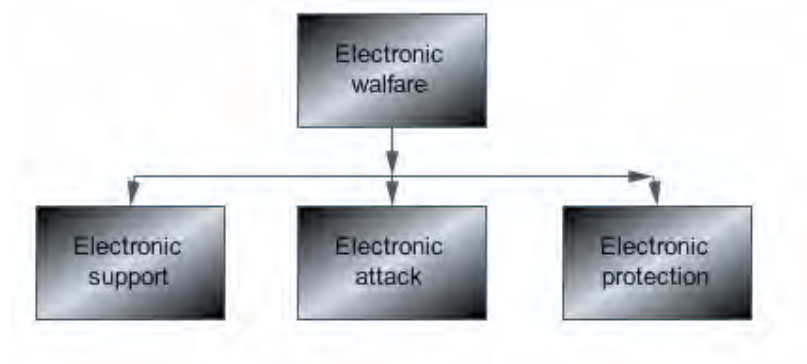


Figure 2.1 *Components of EW*

2.2 Radar

Radar was developed to detect and track aircraft and ships so that they could be attacked. Now there are a wide variety of radars for both peaceful and warlike purposes. For example, radars track aircraft for air-traffic control, determine weather conditions, map ground contours, track ships or surface vehicles, and detect people moving over terrain [2, 6].

2.2.1 Radar Modulation and Parameters

Radar Modulation

Modulation is “the process by which some characteristic of the carrier is varied in accordance with a modulating wave” and the result of that process. A modulator is the device that imposes modulation on the carrier.

In radar applications three basic types of modulation are used: amplitude modulation, frequency modulation, and phase modulation.

- **Amplitude modulation** is “the process by which a continuous high-frequency wave (carrier) is caused to vary in amplitude by the action of another wave containing information.”
- **Frequency modulation** changes the carrier frequency gradually in time in accordance with the modulating signal.
 - **Frequency-modulation-by-noise** is frequency modulation with random noise, as used in ECM to jam victim radars, especially those using amplitude modulation and fixed-tuned frequency modulation receivers.
- **Phase modulation** causes the phase and carrier frequency to vary in accordance with the modulating signal [25].

Radar Parameters

- **Pulse Width:** Duration of the pulse. The amount of time that the radar transmitter is ON. Important in determining range resolution, minimum and maximum range of the radar. It is measured in units of time
- **Pulse Repetition Interval:** time Pulses are usually transmitted at a regular interval, known as the *pulse repetition interval* (PRI) shown Figure 2.2.

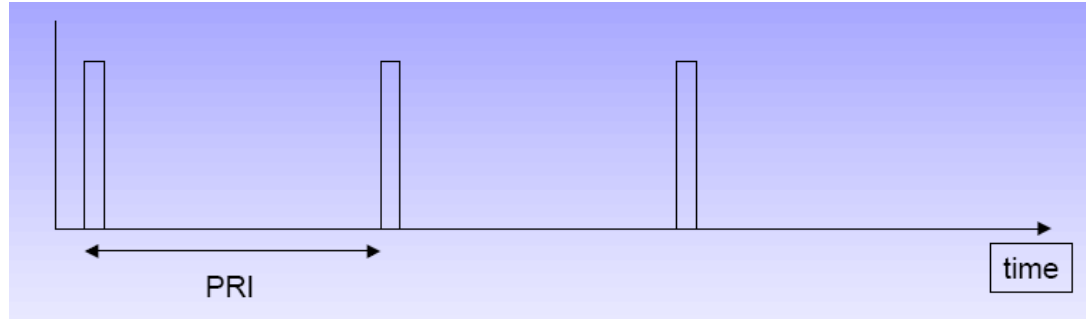


Figure 2.2 *pulse repetition frequency*

- **Pulse Repetition Frequency:** Frequency of the pulse transmission affects the maximum range that can be displayed. $PRF=1/PRT$. The elapsed time between the beginning of one pulse transmission and the beginning of the next. **PRF** is the number of pulses per sec. Normally measure/expresses in Hz.

2.2.2 Frequency Used for Radar

Today, radars of various kinds operate at frequencies ranging from at low as a few megahertz to as high as 300,000,000 megahertz .At low end are a few highly specialized radars: sounders that measure the height of the ionosphere, as well as radars that take advantage of ionosphere reflection to see over the horizon and detect targets thousands of miles away. At the high end are laser radars, which operate in the visible region of the spectrum and are used to provide the angular resolution needed for such tasks as measuring the ranges of individual targets on the battlefield. Most radar, however, employ frequencies lying some where between a few hundred megahertz and 100,000 megahertz [22].

2.2.3 The Radar Cross Section of a Target

The amount of energy reflected to the radar receiver from a target depends on the radar cross section (RCS) of the target. In radar equations, the RCS is usually represented by the symbol σ . RCS is typically defined for monostatic radars, but for bistatic radars there is also a bistatic RCS. RCS is a function of the geometric cross section of the target, its reflectivity, and its directivity. Most fighter strike aircraft have low RCS, which range from under 1m^2 to 10m^2 for head-on aspect ; for this study , the minimum RCS has been selected, since UAV by it self one of the target for a radar [1, 13, 29].

2.2.4 Types of Radars

We will classify radars in terms of the tasks that they perform. Each radar type has characteristics that strongly affect the way it interacts with EW systems, and hence the way they are represented in EW modelling and simulation.

Tracking Radars

A tracking radar system measures the coordination of a target and provides data which may be used to determine the target path and to predict its future position.

Tracking radars provide sufficiently high location accuracy and frequent location updates to allow weapons to engage their targets. Radar guided missiles are actually guided to the constantly updated locations of their targets.

Tracking radars typically operate at higher frequencies than search radars. They also have shorter pulses and higher pulse repetition rates. They are designed to operate over a little more than the lethal range of the weapons they support [2].

Search Radars

Air search radars are sometimes called EW radars because of their roles in early warning and ground control intercept. These radars typically have very long range. They are at relatively low frequencies and have long pulse duration. Some search radars have *chirped* pulses (i.e., pulses with linear frequency modulation). This allows the range resolution of the radar to be improved. Range resolution can also be improved through the use of binary codes during the pulse. Search radar antennas are usually large, providing relatively narrow antenna beams [13].

The thesis focused about P-15 search radar which is found in many countries including East Africa. The detail technical specification has shown Appendix A.

2.2.5 Radar Performance

Radar performance is described in terms of several important equations, listed below

- The radar range equation yields the signal level received by a radar receiver as a function of the transmitter power, the antenna gain, the range to the target, the operating frequency, and the RCS of the target.

- The detection range of the radar is the range at which the radar can achieve sufficient signal in its receiver to adequately measure the range and angle(s) to a target of a specific RCS level. This equation is derived from the radar range equation.
- The delectability range of the radar is the range at which a hostile receiver can detect the radar's signal. This must be defined in terms of the performance specifications of the receiver [8].

2.3 Electronic Attack

Throughout history, military warfare has been about measures to defeat one's enemy and counter measures to those measures on the other side. In modern times, nowhere is this more evident than in IW (information warfare). EW practices are always undergoing changes due to an adversary changing their capabilities based on a countermeasure development by the other side [3, 14].

2.3.1 EA Effect on Radar

To understand the philosophy of EA design, it is necessary to consider the effects of EA on the victim radar. These effects and the deployment of EA are different for surveillance and tracking radar, so it is natural to discuss these radar types separately.

The Effect of EA on Surveillance Radar

Usually, military surveillance radar must provides three-dimensional information for an air search and two-dimensional data for a surface or when a dedicated height-finding radar is coordinated with the air search or when a dedicated height-finding radar is coordinated with the air search radar. Radar data are naturally in spherical coordinates (e.g., range, azimuth, and elevation).

Use of noise jamming in either support or self-screening modes attempts to conceal both the magnitude and direction of a raid. When deployed from a stand-off/stand-in jammer with a quiet attack aircraft, it is possible to completely conceal the raid's direction until a late stage of the operation.

Against surveillance radar's principal tactic is to generate a sufficient number of false targets to overload the radar's data processing system. The jammer, by generating deceptive pulse whose amplitude is inverse of the incident radar signal and sufficient to penetrate the radar's side lobe structure, which can deny the radar to detect the signal but the use of received

jamming signal helps as an indicator of the direction of the jamming aircraft. This inverse gain jamming when used on-board the protected aircraft can confuse the direction of the attack and its intensity. The use of staggered pulse repetition frequency (PRF) on the surveillance radar causes all false targets to occur at ranges greater than the jamming aircraft, but sufficient confusion can generally be generated by this form of jamming to deny an accurate estimate of raid size [25].

The Effect of EA on Tracking Radar

Self-protection ECM systems to counter tracking radar tend to use deceptive EA types of techniques. This reflects a strategy of attempting to cause the tracking radar to break lock rather than have the penetrate mask its own position through noise jamming. Noise jamming is somewhat suspect against tracking radar because the potential for tracking the EA radiations in angle (track-on-jam) always exists. In addition, angle tracking is sufficient, to a first order, for a missile system that uses semi active guidance. Also, multiple angle-tracking radars have the potential for computing range using triangulation techniques. The detail principles are beyond the scope of this thesis [25].

2.4 Jamming

Jamming is the intentional emission of [radio frequency](#) signals to interfere with the operation of a radar or communication radio by saturating its receiver with [noise](#) or false information.

Figure 2.3 shows the radar-jamming concept. The jammer places a signal into the radar receiver that interferes with the reception or processing of the reflected signals returning from the target. For bistatic radar, you need to put the jamming signal into the receiver location [9, 14].

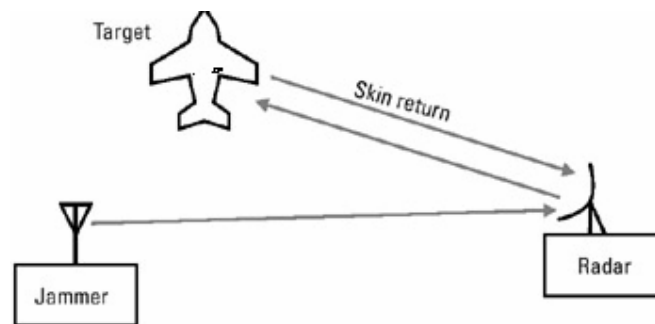


Figure 2.3 Radar-jamming geometry

Jamming can be classified by type of threat signal (radar versus communication), by jamming geometry (standoff versus self-protection), and by jamming technique (cover versus deceptive versus decoy). While it is somewhat controversial to include decoys as a type of jamming, they act a lot like jammers and their performance is calculated using some of the same equations.

2.4.1 Radar Jamming

For radar jamming, consider the diagram shown in Figure 2.4. The J/S is the ratio of the power of the jammer that gets into the radar receiver to the power of the skin return in the radar receiver. There are several complicating factors to consider. First, we must consider the radar antenna directivity. The radar antenna is pointed at the target, so the skin return is increased twice by the gain of the antenna (once during transmission and once during reception). The transmitted jamming signal is increased by the jammer antenna gain (not the radar antenna gain) and is increased by receiving gain of the radar antenna only if the jammer is located on the target. Otherwise, the jammer must enter the radar antenna through its side lobes, which have much less antenna gain.

Another complicating factor is that the skin return to the radar is reduced by the fourth power of the distance from the radar to the target, while the jamming signal is only reduced by the square of the jammer to radar receiver distance.

Thus, as summarized in the J/S for radar jamming is a function of the fourth power of the distance to the target divided by the square of the distance to the jammer. It is also a function of the radiated jammer power to the radiated radar power and the ratio of the radar side lobe power to main beam power. The final factor is the RCS of the target. All else being the same, the smaller the RCS, the larger the J/S . All detail described in chapter Four [8, 25].

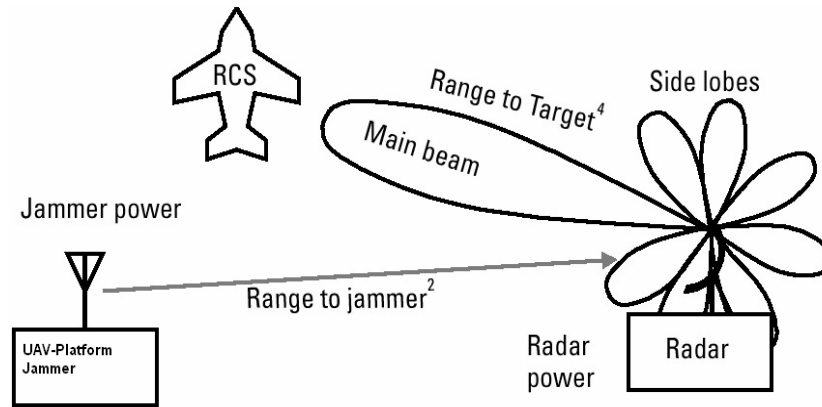


Figure 2.4 Radar-jamming J/S factors.

2.4.1.1 Jamming Tactics: Three Standard Tactics are used:

Stand-off and Stand-in Jamming

Support ECM is ECM radiated from one platform and is used to protect other platforms. Figure 2.5 illustrates two cases of support jamming: stand-off jamming (SOJ) and stand-in jamming (SIJ). For SOJ the support jamming platform is maintaining an orbit at a long range from the radar – usually beyond weapons range (Usually greater than 60Km). For SIJ, a remotely piloted vehicle is orbiting very close to the victim radar, for this study the effect of jamming from 130 Km to 50 K from the victim radar, including crossover range have been described [8,25].

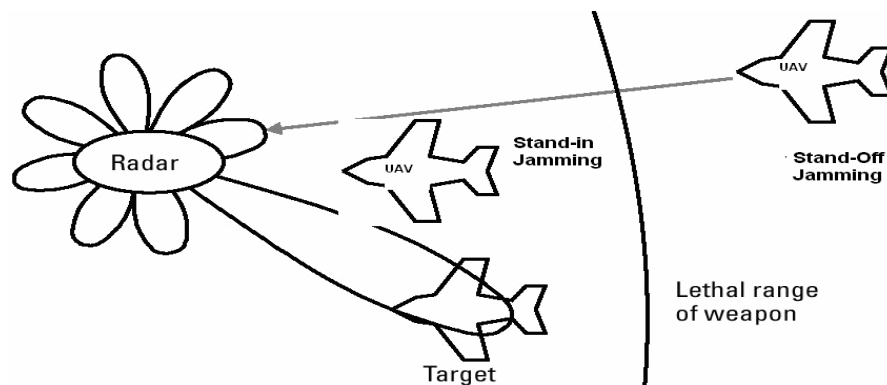


Figure 2.5 Stand-off and Stand-in jamming geometry

Self-protection Jamming

In self-protection jamming, the jammer is, by definition, located on the target (see figure 2.6). Thus the jammer has the advantage, being no farther from the radar than the target. It is also

amplified by the radar's main beam gain. With these advantages, the self-protection jammer has sufficient power to break the lock of radar that is tracking the target [8, 25].

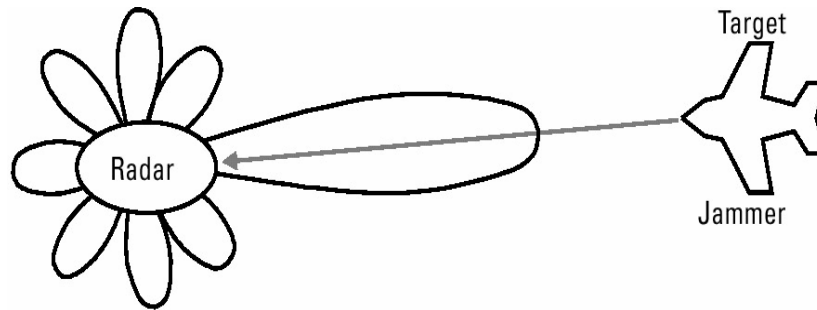


Figure 2.6 *Self-protection jamming geometry*

2.4.1.2 Noise Jamming

The objective of noise jamming is masking the actual signal. In principle, noise jamming increases the radar receiver noise level and the jamming signal has the characteristics of receiver noise [25]. Gaussian noise is the best noise-jamming waveform. This follows because white Gaussian noise has the maximum entropy, or uncertainty of any random waveform for a specific average power [14] and it provides a constant power spectral density [20].

One-way of preventing a radar receiver from functioning correctly is to saturate it with noise. Noise is a continuous random signal and is dissimilar to radar signal. The radar signal or echo is a periodic sequence of pulses. The objective is to conceal the radar echo. This idea can be alternatively expressed by saying that the average power of the jammer must have the same effect as the peak power of the radar echo, or by saying that the noise-to-signal ratio at the input is raised to a level beyond which the receiver can extract intelligence. The effect of noise jamming on PPI shown Figure 2.7 [22] and the detail mathematical equation can be found chapter Four (4.2.2) .

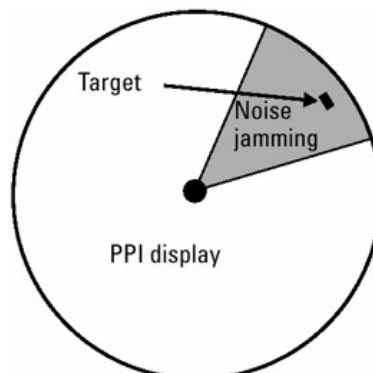
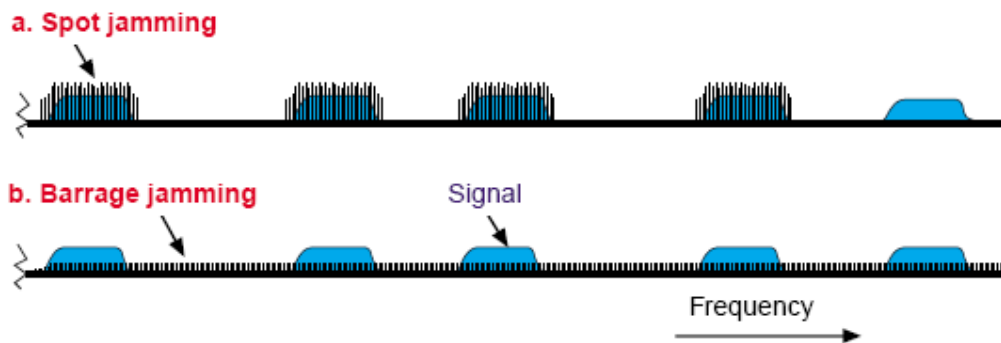


Figure 2.7 *Noise jamming on a PPI display*

As shown in the figure 2.7 the radar PPI (plan position indicator) covered by noise signal so that the radar can not detect the target echo signal effectively.

Major Noise Jamming Techniques: Within the general class of jamming, there are three different techniques for generating the noise like signal. In **spot jamming** all the power output of the jammer is concentrated in a very **narrow bandwidth**, ideally identical to that of the radar as shown Fig.2.8a. **Barrage jamming** spread their energy over a bandwidth must wider than that of the radar signal. Thus, spot jamming is usually directed against specific radar and requires a panoramic receiver to match the jamming signal to the radar signal. The other techniques, however, can be against any number of radars and only require receiver to tell them that there is radar present [22, 27]. Since the UAV-Platform jammer attack specific frequency, the analysis is based on spot jammer.

Figure 2.8 *Spot and Barrage jamming*

2.5 UAV (Unmanned Aerial Vehicles)

The development of uninhabited aerial vehicles (UAVs) raises the possibility of states that will be able to conduct military operations in a more efficient with less risk than that of an aircraft piloted by humans.

As a result of numerous technological developments, it is possible that the Ethiopia will be able to build military systems, including UAVs, which can conduct military operations without human intervention. UAV can be used to augment the collection capability of the high-flying system [3].

A number of technological factors suggest that unmanned weapon systems will be

important in future military operations. To understand how the technology behind the development of UAVs is changing the nature and conduct of military operations, this thesis examines the role of UAV on military operation.

2.5.1 Categorizing Military Operations

The roles of UAVs can vary widely based on the difficulty of the military operation that is to be conducted. The simplest military operations involve attacks against fixed ground targets, while the more challenging operations involve attacks against mobile ground targets and other air vehicles. As one would expect, an attack against fixed targets is the simplest because it is relatively easy to find targets whose location does not vary and which can be assessed with great accuracy. However, an attack against air targets is more difficult because the target's mobility makes it more difficult to find and destroy the target, and further because the target's ability to maneuver makes it more difficult to prosecute an attack. Even when an air target has been located, the simplest form of attack is the unobserved attack in which the target is not aware that it is under attack.

By contrast, an observed attack against a highly maneuverable target even with an experienced pilot is most difficult.

There are various type of UAV which are used for EW, among this: Global Hawk, Predator UAV, and Hunter UAV are most familiar [14]. This thesis focused on **Predator –UAV**.

2.5.2 Predator UAV

The Predator UAV is classified as a medium altitude endurance platform and operates at 26000ft; remaining on station for up to 40 hrs at a distance of 250Km from the base .This UAV can carry a radar jammer [3, 14]. Their technical specifications are shown in table 2.1.

Predator UAV Technical Specification

UAV-parameter	Amount	Unit
Range	250	Km
Endurance	20	hrs
Payload	450	lbs
Max altitude	26000	ft
Length	8.2	m

Power available	3	Kw
Cruise Speed	80	mph

Table 2.1 *UAV Technical Specification*

CHAPTER 3

UAV-PLATFORM JAMMER

3.1 Introduction

A jammer can be deployed in various platforms. In that case, it might be delivered to its operating site by a soldier who emplaces it by hand, or it might be delivered by some other means such as deployed from a UAV or shot into place out of an artillery cannon or rocket.

3.2 Simplified Block Diagram of a Jammer

The Figure 3.1 shows a block diagram of a jammer [5, 6, 7, 15, 16, 27]. The RF-carrier comes in from the antenna and is applied to a filter. The output of the filter is only the frequencies of the desired frequency-band. These frequencies are applied to the mixer stage. The mixer also receives an input from the local oscillator. These two signals are beat together to obtain the IF through the process of heterodyning. The IF-carrier is applied to the IF-amplifier. The amplified IF is then sent to the Match filter for optimal detector. The output of the detector analyzed at radar signal parameter measurement. After decision (at Command and Control circuit) this signal can be used as an input for jammer transmitter.

A signal classifier performs measurements on an IF signal and determines from these measurements the nature of the modulation, if any, appearing on a received high frequency radar signal. The classifier distinguishes modulation type, unmodulated carrier and noise in short signal classification is used to detection, pattern recognition and decision making system [23, 21].

Parameter Measured by Jammer System: Each instantaneous signal intercepted by the jammer system must be characterized by a set of parameters. This provides the information required to associate a set of signals belonging to a particular emitter and to identify that emitter among other emitters whose signals have been intercepted. The parameters generally measured by the jammer system are carrier (RF) frequency, pulse amplitude (PA), pulse width (PW), and angle of arrival (AOA) [22, 26, 30].

Once a signal is isolated, another set of signal parameters associated with the emitter can be determined which include the PRF, antenna scan rate or type, and range.

Channel processing (not shown the block diagram) is used to isolate the active signal from each IF channel, and then correlate these signal against the current threat UAV database received from the wideband analysis system to identify active threat signal.

If a threat signal is identified, a jamming signal is created at DDS (direct digital synthesizer) and the jammer modulator can mix this signal and jammer noise signal (Gaussian). The desired output power can be provide at power amplifier (it provides 50 watt for Stand-off, and 6.3 watt for stand-in jammer, the detail analysis can be found chapter Six). The entire desired jammer signal is radiated toward the victim radar [14].

Coordination of this processing section is facilitated through command and control element consisting of a finite state machine and a number of control ports. This control element typically maintains the UAV database, which has predefined the necessary data before take off, and is used to dynamically load and unload jamming modulation schemes.

Based on the functional partition of jamming system shown Figure 3.1, the hardware can be portioned as follows: [4, 24]

- Transmitter
- Transmitting and Receiving antenna
- Propagation path to target
- Propagation path-target to receiver
- Controllable element
- Power Supply

3.3 Jammer Receiver and Transmitter

Jammer Receiver

Consider the input signal which has the following voltage waveform [6]

$$S_{in}(t) = Ap(t) \cos(w_o t + \varphi(t)) \quad (3.1)$$

Where $p(t)$ is the pulse waveform and w_o is the radar frequency

The local oscillator generates a signal

$$S_{LO}(t) = A_{LO} \cos[(w_{RF} - \varphi(t)] \quad (3.2)$$

Where w_{IF} , the “**intermediate frequency,**” is a frequency much lower than the RF. The output of RF amplifier is combined with the local signal $S_{LO}(t)$ of (3.2) in a way that results in

a signal at the IF whose slowly varying amplitude with undistorted phase. IF signal is much easier to amplify and to work with than that of the RF signal.

The action of the mixer is basically an addition of the local oscillator signal with the output of RF amplifier followed by a non-linear detector .The RF amplifier output is

$$S_{RF}(t) = ap(t) \cos[w_{RF}t + \varphi(t)] \quad (3.3)$$

Where again $p(t)$ and $\varphi(t)$ are slowly varying compared with $\cos w_o$ or $\sin w_o$, where w_o denotes either w_{RF} or w_{IF} .

Adding $s_{RF}(t)$ as in (3.3) and $S_{LO}(t)$ as in (3.2) and squaring the result, we would obtain

$$\begin{aligned} [s_{RF}(t) + s_{LO}(t)]^2 &= \frac{a^2 p^2(t)}{2} [1 + \cos[2w_{RF}t + 2\varphi(t)]] + \frac{A_{LO}^2}{2} [1 + \cos[2(w_{RF} - w_{IF})t]] \\ &+ \frac{2A_{LO}ap(t)}{2} [1 + \cos[(2w_{RF}t - w_{IF})t + \varphi(t)]] + \cos[w_{IF}t + \varphi(t) = s_1(t) + s_2(t)] \\ &+ s_3(t) + s_4(t) + s_5(t) \end{aligned} \quad (3.4)$$

Where

$$s_1(t) = \frac{a^2 p^2(t)}{2} + \frac{A_{LO}^2}{2} \quad (3.5)$$

$$s_2(t) = \frac{A_{LO}^2}{2} [1 + \cos[2(w_{RF} - w_{IF})t]] \quad (3.6)$$

$$s_3(t) = \frac{2A_{LO}ap(t)}{2} \cos[(2w_{RF}t - w_{IF})t + \varphi(t)] \quad (3.7)$$

$$s_4(t) = \frac{a^2 p^2(t)}{2} \cos[2w_{RF}t + 2\varphi(t)] \quad (3.8)$$

$$s_5(t) = A_{LO}ap(t) \cos[w_{IF}t + \varphi(t)] \quad (3.9)$$

One of the five mixer output signal selected for IF. The spectra of the other four signals $S_1(t), S_2(t), S_3(t)$ and $S_4(t)$ are centered, respectively, at DC (far below IF), $2(w_{RF}-w_{IF})$ (for above IF, near RF), $(2w_{RF}-w_{IF})$ (still further above IF, near twice the RF), and $2w_{RF}$ (twice the RF, still further above IF). The net result of all this is that the IF amplifier, whose passband is centered at IF and whose bandwidth is generally about 10 to 20% of IF, passes only $S_5(t)$ and reject all

of the other five signals [4,13,23]. The IF of P-15 radar has 10 to 20 MHz and by taking 10 MHz, the corresponding local oscillator frequency generates 760MHz for the jammer system.

Matched filters

A matched filter is a filter that provides the maximum output SNR when the signal is corrupted by white Gaussian noise. White noise means the power spectrum of the noise $P_n(f)$ is uniformly distributed over the entire frequency domain ($-\infty < f < \infty$) (i.e., $P_n(f) = N_0/2$), and Gaussian noise indicates that the probability density function of the amplitude of the noise is a Gaussian distribution. Given a signal $s(t)$ in white Gaussian noise, the transfer function of the matched filter is the complex conjugate spectrum of the time-shifted signal $s(t + t_0)$:

$$H(f) = kS^*(f) \exp \{-j2\pi f t_0\} \tag{3.10a}$$

and its impulse response is a mirror function of the input signal

$$h(t) = \begin{cases} Ks^*(t_0 - t), & (t \geq 0) \\ 0, & (t < 0) \end{cases} \tag{3.10b}$$

where t_0 is a predetermined observation time and k is a scaling constant.

The matched filter has many important properties:

- Among all linear filters, the matched filter is the only one that can provide maximum output SNR of $2E/N_0$, where

$$E = \int_{-\infty}^{\infty} s^2(t) dt$$

the energy of the signal $s(t)$, and $N_0/2$ is the power spectrum density of the white noise.

- An optimal filter matched to the signal $s(t)$ is also optimum to those signals that share the same waveform but different magnitude and time delay: $s'(t) = as(t - \tau)$;
- The matched filter is equivalent to a correlator. Because the impulse response of the matched filter is a mirror of the input signal, the output of the matched filter can be expressed as an autocorrelation function of the signal [28].

For uncompressed pulse there are two cases: [18, 31]

- Rectangular received pulse passing through a rectangular filter

Output signal-to-noise ratio at this width relative to a matched filter: 0.825

Loss at the optimum filter width relative to a matched filter 0.838 dB

- Rectangular received pulse passing through a Gaussian shaped filter
 Output signal-to-noise ratio at this width relative to a matched filter: 0.89
 Loss at the optimum filter width relative to a matched filter 0.506 dB

However for the study focused on the first case only even if a Gaussian shaped filter is a good performance than rectangular filter, so as to create the worst condition for the jammer.

Jammer Transmitter

Consider the block diagram Figure 3.1 the symbol $s_k(t, \Omega_k)$ denotes the jammer/radar signal waveform. The symbol Ω_k represents a vector containing parameters such as amplitude, path delay, frequency, and phase due to causes other than path delay.

The brief discussion of the action of each constituent in changing the signal from $s_{k-1}(t, \Omega_{k-1})$ to $s_k(t, \Omega_k)$, where the index on Ω refers to the numbered “stage” of the signal flow at jammer transmitter sub- topic is explained below.

Now assume the $s_1(t; \Omega_1)$ is the out put of the jammer power amplifier and hence this signal $s_1(t; \Omega_1)$ entering the transmission line on its way to the transmitting antenna has the generic form

$$s_1(t; \Omega_1) = A_T a_M(t) \cos[w_o t + \varphi_T(t)] \tag{3.11}$$

Where A_T is the amplitude of the signal, $a_M(t)$ is the waveform representing the normalized (to A_T) form of the time varying amplitude of the transmitted signal, and the function $\varphi_T(t)$ is the phase shift induced by the modulation waveform. The time variation of $a_M(t)$ and $\varphi_T(t)$ are large compared with $\cos(w_o t)$ or $\sin(w_o t)$, or equivalently a waveform of the form (3.11) is known as a “wider band” signal. This means that the modulation bandwidth is larger compared with the radar bandwidth; the bandwidth of the jammer is found in chapter four. Alternatively we could represent (3.11) with two “quadrature” component $x_1(t; \Omega_1)$ and $y_1(t; \Omega_1)$ or

$$s_1(t; \Omega_1) = x_1(t; \Omega_1) \cos w_o t + y_1(t; \Omega_1) \sin w_o t \tag{3.12}$$

Where

$$x_1(t; \Omega_1) = A_T a_M(t) \cos[\varphi_T(t)]$$

$$y_1(t; \Omega_1) = -A_T a_M(t) \sin[\varphi_T(t)]$$

Or in the form

$$s_1(t; \Omega_1) = \text{Re}[\hat{\mathcal{S}}_1(t; \Omega_1) e^{j\omega_o t}] \quad (3.13)$$

Where

$$\hat{\mathcal{S}}_1(t; \Omega_1) = A_T a_M(t) e^{j\varphi_T(t)} \text{=} \text{“Complex envelope” of the signal } s_1(t; \Omega_1)$$

and where it is recognized from (3.12) and (3.13) that

$$x_1(t; \Omega_1) = \text{Re}[\hat{\mathcal{S}}_1(t; \Omega_1)] \quad y_1(t; \Omega_1) = -\text{Im}[\hat{\mathcal{S}}_1(t; \Omega_1)]$$

3.4 The Transmission Antenna

The transmission leading from the output of the RF power source to the input terminals of the antenna, which produces the electrical field components at the antennas aperture that have the form of:

$$s_2(t; \Omega_2) = a_2(t) \cos[\omega_o t + \varphi_2(t)] \quad (3.14)$$

Where

$$\begin{aligned} a_2(t) &= K_{12} A_T a_M(t) \\ \varphi_2(t) &= \varphi_T(t) + \Delta\varphi_{12} \end{aligned}$$

And where k_{12} is an amplitude scale factor due to the line and antenna (generally a loss, due to reflection at the termination and mismatch between the antenna impedance and that of free space) and $\Delta\varphi_{12}$ is the phase shift introduced by the line-antenna network. Equation (3.14) indicates simply that the network, being linear, can change the amplitude scale and shift the phase of the signal entering it but will not change the frequency ω_o or distort the slowly varying functions $a_M(t)$ and $\varphi_T(t)$ [23].

3.5 The Propagation Path to Radar

The next stage of the signal's journey is the propagation path from transmitter to victim radar. It is assumed that the path is entirely in free space. That is the idealization that facilitates qualitative thinking about radar, and is the logical place to begin the analysis of a radar system.

If the path is entirely in “infinite” free space, then the only effect of that path is to introduce a time delay $\tau_{d1} = r/c$ and a possible Doppler shift $w_{d1} = \omega_o V_{rel} / c$ where V_{rel} is the relative

line-of-sight velocity component between transmitter and target. Thus the signal waveform appearing at the radar is given by

$$s_3(t; \Omega_3) = a_3(t - \tau_{d1}) \cos[(w_o + w_{d1})(t - \tau_{d1}) + \varphi_3(t - \tau_{d1})] \quad (3.15)$$

Where $a_3(t) = (K_{23}/r)a_2(t)$, $\varphi_3(t - \tau_{d1}) = \varphi_2(t - \tau_{d1})$, the phase shift incurred in the transmitter and its antenna, and where K_{23} is a scale factor due to the antenna pattern and the $\frac{1}{r}$ loss in the field strength(translating into a $1/r^2$ power loss) accounted for [23].

At the radar receiving Antenna

The receiving antenna performs a linear transformation on-the signal impinging on it, i.e., an amplitude loss k_{56} and a fixed phase shift $\Delta\varphi_{56}$. The result is

$$s_4(t; \Omega_4) = a_4(t - \tau_d) \cos[(w_o + w_d)(t - \tau_d) + \varphi_4(t - \tau_d)] \quad (3.16)$$

Where

$$a_4(t) = k_{34}a_3(t)$$

$$\varphi_4(t - \tau_d) = \varphi_3(t - \tau_d) + \Delta\varphi_{34}$$

The latency between the times a signal is detected and the time that the jammer signal is transmitted toward the victim radar must typically be very small, often times less than a few microseconds, to provide effective jamming of short duration of frequency agile signal.

3.6. Jammer Losses

As indicated by the jammer EIRP equation (Eq.4.24), the receiver EIRP_J is inversely proportional to the jammer losses. Hence, any increase in jammer losses causes a drop in the EIRP_J, thus decreasing the probability of detection, as it is a function of the SNR. Jammer losses include ohmic (resistance) losses and statistical losses. In this thesis we can find the jammer fluctuation loss and integration loss using matlab tool, other loss can be taken at standard reference material [1].

3.6.1 Transmit and Receive Losses

Transmit and receive losses occur between the jammer transmitter and antenna input port, and between the antenna output port and the receiver front end, respectively. Such losses are often called plumbing losses. Typically, plumbing losses are on the order of 1 to 2 dB [13].

3.6.2. Atmospheric Loss

Atmospheric attenuation is a function of the jammer operating frequency, target range, and elevation angle [13]

3.6.3. Processing Losses

Detector Approximation: The output voltage signal of a radar receiver that utilizes a linear detector is

$$v(t) = \sqrt{v_I^2(t) + v_Q^2(t)} \quad (3.17)$$

Where (V_I , V_Q) are the in-phase and quadrature components. For jammer using a square law detector, we have $V^2(t) = V_I^2(t) + V_Q^2(t)$.

Since in real hardware the operations of squares and square roots are time consuming, many algorithms have been developed for detector approximation. This approximation results in a loss of the signal power, typically 0.5 to 1 dB.

The jammer fluctuation and Integration loss can be found using simulation result in chapter 5. Other loss can be taken from standard reference document using the Ethiopia weather condition and considering the worst case .For radar case I used only 8dB (Note: the detail can be found chapter 4) so as to provide optimal detection for the radar receiver. The jammer loss can be summarized in table (3.1) [2, 13, 18]

No	Jammer loss	dB
1	Integration loss	2.2
2	Fluctuation losses	4.5
3	Filter matching loss	0.83
4	Atmospheric loss	1
5	Processing losses	1
6	Transmitter and Receiver loss	2
7	Beam width factor	1
8	Troposphere loss(Using UAV altitude height)	0.6
9	Rain fall loss(Ethiopia rain fall, 10mm/hr at 750Mhz frequency)	0.4
10	Attenuation at 5 ⁰ elevation and 750MHz frequency	0.6
	Total	14.1

Table 3.1 Jammer Loss

CHAPTER 4

JAMMER EQUATION

4.1 The Radar Equation

So as to develop the jammer equation first we consider the radar equation .Let us reconsider the power budget of the link (in free space range [36]): a radar transmitting power P_t in the direction of a target located at distance R with an antenna gain of G_t .

The power density at the target is as follows [13]:

$$W = G_t \frac{P_t}{4\pi R^2} \quad (4.1)$$

The power received by the target is $P_c = W \sigma$, where σ is the effective area of the target considered as receiving antenna. The target diffuses this power isotropically in accordance with the mode.

The power received by the radar receiver antenna, which has an effective area S_{ef} , is [13]

$$P_r = \frac{P_c}{4\pi R^2} S_{ef}, \quad (4.2)$$

Giving the power budget

$$P_r = P_t \frac{G_t S_{ef} \sigma}{(4\pi)^2 R^4} \quad (4.3)$$

Replacing S_{ef} with $\frac{G_r \lambda^2}{4\pi}$ yields the power budget [13]

$$P_r = P_t \frac{G_t G_r \lambda^2 \sigma}{(4\pi)^3 R^4}. \quad (4.4)$$

REMARKS

- For a monostatic radar like P-15 (one that uses the same antenna for transmission and reception),[13]

$$G_t = G_r = G$$

- P_t and P_r designate either peak power and mean power.

Let S_{\min} denote the minimum detectable signal power. It follows that the maximum radar range R_{\max} is [22]

$$R_{\max} = \left(\frac{P_t G^2 \lambda^2 \sigma}{(4\pi)^3 S_{\min}} \right)^{1/4} \quad (4.5)$$

Eq. (4.5) suggests that in order to double the radar maximum range one must increase the peak transmitted power P_t sixteen times; or equivalently, one must increase the effective aperture four times.

In practical situations the returned signals received by the radar will be corrupted by the noise, which introduces unwanted voltages at all radar frequencies. Noise is random in nature and can be described by its Power Spectral Density (PSD) function. For a receiver of bandwidth B and a temperature T_e (in Kelvin, K), this noise is quantified as [1]

$$N = \text{NoisePSD} \times B \quad (4.6)$$

The input noise power to a lossless antenna is

$$N_i = kT_e B \quad (4.7)$$

Where $k=1.38 \times 10^{-23}$ joule/degree Kelvin is Boltzman's constant, and $1K=273+T(^{\circ}C)$. It is always desirable that the minimum detectable signal (S_{\min}) be greater than the noise power. The fidelity of a radar receiver is normally described by a figure of merit called the noise figure. The noise figure is defined as [13, 22].

$$F = \frac{(SNR)_i}{(SNR)_o} = \frac{S_i / N_i}{S_o / N_o} \quad (4.8)$$

$(SNR)_i$ and $(SNR)_o$ are, respectively, the Signal to Noise Ratios (SNR) at the input and output of the receiver. S_i is the input signal power; N_i is the input noise power, S_o and N_o are output signal and noise powers respectively. Substituting Eq. (4.7) into Eq.(4.8) and rearranging terms yields [1]

$$S_i = kT_e B F (SNR)_o \quad (4.9)$$

Thus, the minimum detectable signal power can be written as [2]

$$S_{\min} = kT_e B F (SNR)_{o \min} \quad (4.10)$$

The radar detection threshold is set equal to the minimum output SNR, $(SNR)_{0\min}$. Substituting Eq.(4.10) in Eq. (4.5) gives

$$R_{\max} = \left(\frac{P_t G^2 \lambda^2 \sigma}{(4\pi)^3 K T_e B F (SNR)_{0\min}} \right)^{1/4} \quad (4.11)$$

Or equivalently, [1]

$$(SNR)_{0\min} = \frac{P_t G^2 \lambda^2 \sigma}{(4\pi)^3 K T_e B F R_{\max}^4} \quad (4.12)$$

Sources of S/N loss include ohmic and non-ohmic (mismatch) loss in the antenna and other radio frequency components, propagation effects, signal processing deviations from matched filter operation, detection threshold, and search losses. Search operations (like P-15 radar operation) impose additional losses due to target position uncertainty. Typical loss budgets for several major radar classes are as follows: transmit loss 1.5dB, non-ohmic receiver loss 0.5dB, signal processing loss 1.4dB, beam shape 3dB, range gate straddle 0.5dB, Doppler filter straddle 0.5dB, and detection threshold 1dB [29].

In general, total radar losses denoted as L reduce the overall SNR, and hence [24]

$$(SNR)_0 = \frac{P_t G^2 \lambda^2 \sigma}{(4\pi)^3 K T_e B F L R^4} \quad (4.13a)$$

Although it may take on many different forms, Eq. (4.13a) is what is widely known as the Radar Equation. It is a common practice to perform calculations associated with the radar equation using decibel (dB) arithmetic.

Alternatively, the radar equation can be modified to compute the pulse width required to achieve a certain SNR for a given detection range. In this case the radar equation can be written as [24].

$$\tau = \frac{(4\pi)^3 k T_e F L R^4 SNR}{P_t G^2 \lambda^2 \sigma} \quad (4.13b)$$

The basic jammer parameter can be found by using the above equation and matlab tools as follows:

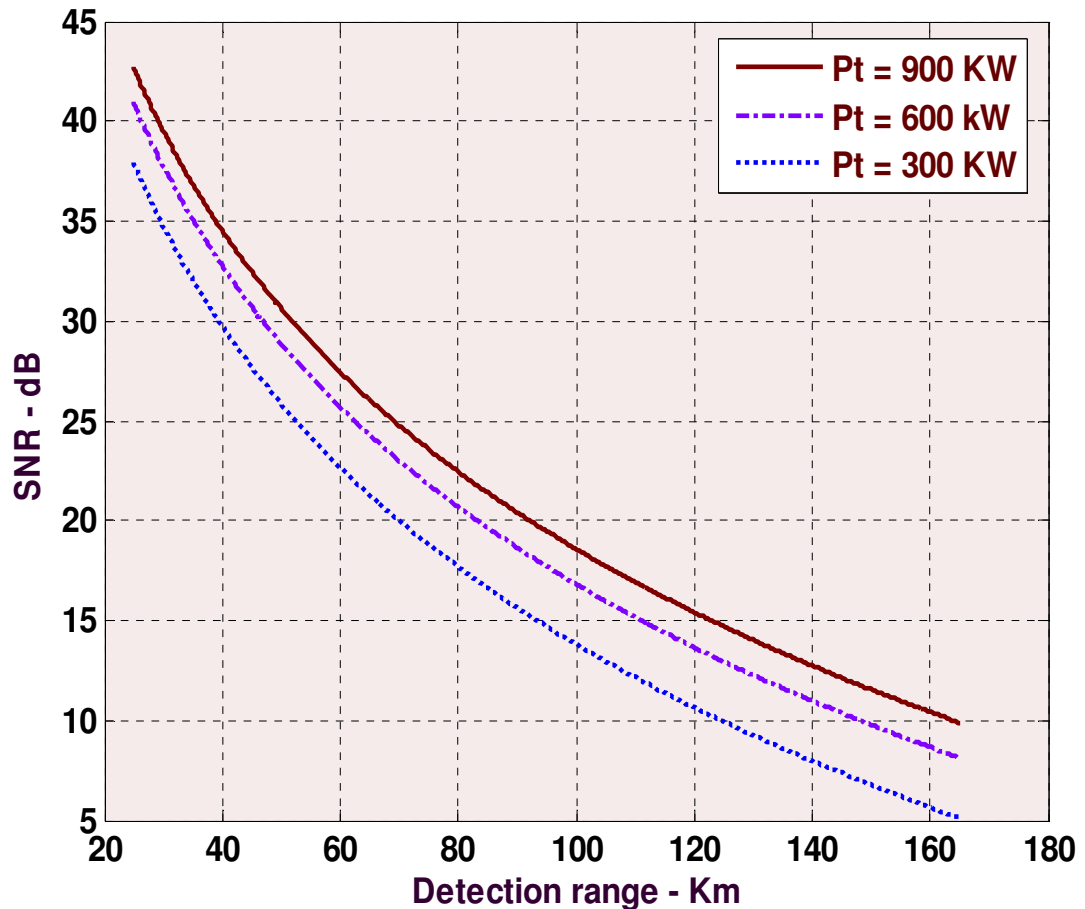


Figure 4.1a SNR versus detection range for three different values of radar peak power.

Figure 4.1a shows the SNR for a given set of radar parameters using equation (4.13a) and the Matlab code can be found in Appendix B. Now assume that the jammer detects at 130Km from the radar, at this point the maximum radar SNR at peak power 900Kw is equal to 14dB.

As experimental analysis shows: $\frac{J}{S} = 5 \text{ dB to } 10 \text{ dB}$ are sufficient to provide significant interference, where J means jammer SNR and S indicates radar SNR [14]. For this thesis $J/S = 8 \text{ dB}$ is considered. Using this concept and the result of the simulation shows the value of $J = 22\text{dB}$. Now considering Pulse-integration Eq. (5.24) and number of integration pulse 10, the

jammer SNR become 12 dB which is the same effect as single pulse used, in addition to that it is more helpful for jammer transmitted power. The detail analysis can be found in chapter 5.

The same result is found using different radar cross section, by selecting $RCS=1m^2$, as shown Fig. (4.1b).

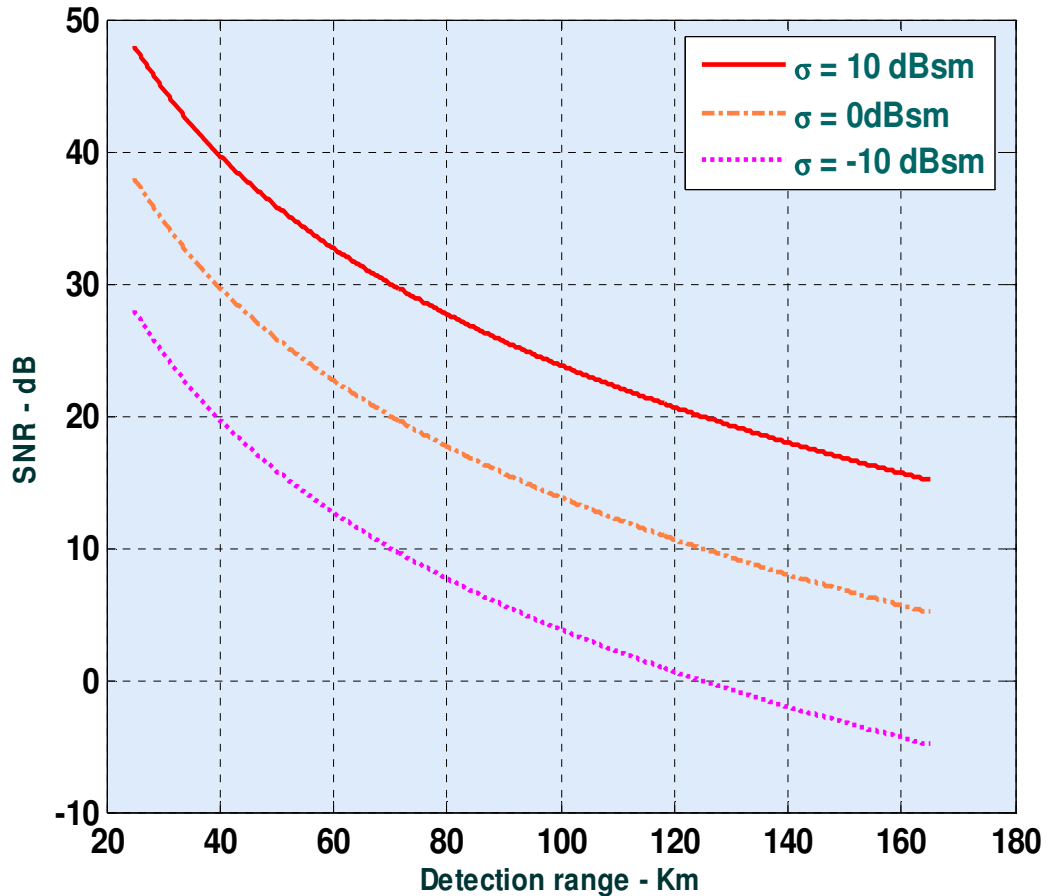


Figure 4.1b SNR versus detection range for three different values of RCS

Figure 4.2 shows an implementation of Eq. (4.13b) for three different detection range values. At 130Km and the SNR equal to 14 dB, the radar pulse width become approximately 2μ second. The actual P-15 radar pulse width become between 2 to 3 μ second, see Appendix A

The radar Bandwidth in this case $B_R = 1/\tau = 0.5\text{MHz}$ [32]. The ratio between the jamming and radar bandwidths (B_J/B_R) is (approx.) 5 for spot jamming.

However if $B_J \gg B_R$, then barrage jamming is used [14]. Since this thesis focused on specific frequency, it used spot jamming, and by taking the $B_J/B_R=4$, the jammer band width equal to 2 MHz



Figure 4.2 Pulse widths versus required SNR for three different detection range values.

4.2 Jammer Equation

A jammer can be identified by its effective operating bandwidth B_J and by its Effective Radiated power (ERP), which is proportional to the jammer transmitter power P_J . More precisely, [6, 14].

$$EIRP = \frac{P_J G_J}{L_J} \quad (4.14)$$

Where G_J is the jammer antenna gain and L_J is the total jammer losses (which are found in table 3.1). The effect of a jammer on radar is measured by the Signal-to-Jammer ratio (S/J).

4.2.1 Self-Screening Jammers (SSJ)

Self-screening jammers, also known as self-protecting jammers and as main beam jammers, are a class of ECM systems carried on the vehicle they are protecting [8,9]. Escort jammers

(carried on vehicles that accompany the attacking vehicles) can also be treated as SSJs if they appear at the same range as that of the target(s). When UAV performs a surveillance operation it can also be used for this type of jamming.

Assume a radar with an antenna gain G , wave-length λ , aperture A_r , bandwidth B_r , receiver losses L , and peak power P_t . The single pulse power received by the radar from a target of RCS (σ) at range R , is

$$S = \frac{P_t G^2 \lambda^2 \sigma \tau}{(4\pi)^3 R^4 L} \quad (4.15)$$

τ is the radar pulse-width. The power received by the radar from an S_{SJ} jammer at the same range is

$$J = \frac{P_J G_J}{4\pi R^2} \frac{A_r}{B_J L_J} \quad (4.16)$$

Where P_J , G_J , B_J , L_J are the jammer's peak power, antenna gain, operating bandwidth, and losses respectively. Using the relation

$$A_r = \frac{\lambda^2 G}{4\pi} \quad (4.17)$$

Then Eq. (4.16) can be written as

$$J = \frac{P_J G_J}{4\pi R^2} \frac{\lambda^2 G}{4\pi B_J L_J} \quad (4.18)$$

Substituting Eq. (4.14) into Eq. (4.18) yields,

$$J = ERP \frac{\lambda^2 G}{(4\pi)^2 R^2} \frac{1}{B_j} \quad (4.19)$$

Thus, S/J ratio for a SSJ case is obtained from Eqs. (4.19) and (4.15),

$$\frac{S}{J} = \frac{P_t G \sigma B_j}{(ERP)(4\pi)R^2 L} \quad (4.20)$$

And when pulse compression is used, with time-bandwidth-product $G_{PC} = B_r \tau$, then Eq. (4.20) can be written as [14]

$$\frac{S}{J} = \frac{P_t G \sigma B_j G_{pc}}{(ERP)(4\pi)R^2 B_r L} \quad (4.21)$$

Note: To obtain Eq. (4.21), one must multiply Eq. (4.20) by the factor B_r/B_r and use the fact that $G_{PC} = B_r \tau$.

4.2.1.1 Burn-through Range

If jamming is employed in the form of Gaussian noise, then the radar receiver has to deal with the jamming signal the same way it deals with noise power in the radar. Thus, detection, tracking, and other functions of the radar signal and data processors are no longer dependent on the SNR. In this case, the S/(J+N) ratio must be calculated. More precisely, [14]

$$\frac{S}{J + N} = \frac{\left(\frac{P_t G \sigma A_r \tau}{(4\pi)^2 R^4 L} \right)}{\left(\frac{(ERP)A_r}{4\pi R^2 B_j} + K T_o \right)} \quad (4.22)$$

Where K is Boltzman's constant and T_o is the effective noise temperature.

4.2.2 Noise Jamming

The objective of noise jamming is to inject an interference signal in to the enemy's electronic equipment such that the actual signal completely submerged by the interference. This type of jamming is also called denial jamming or obscuration jamming. In principle the optimal jamming signal has the same characterises of receiver noise, but in practice this may be difficult to achieve.

The primary advantage of noise jamming is that only minimal details about the enemy equipment need be known. A convenient classification of noise jamming is by the ratio of the jamming signal bandwidth to the acceptance bandwidth of the victim equipment. If the ratio is large, the signal is called barrage jamming, if the ratio is small, the signal is called spot jamming.

To analysis the effect of a noise jamming on search radar, first consider the signal power received by the radar on a signal pulse with out jamming [8, 14]

$$S = \frac{P_T G_T G_R \alpha \lambda^2}{(4\pi)^3 R_t^4 L_R} \quad (4.23)$$

Where,

- P_T =peak power transmitted, W;
- G_T, G_R = transmitter/receiver antenna gain;
- α =RCS, m^2 ;
- λ =wavelength, m;
- R_T = target range, m;
- L_R = radar system losses.

The internal noise power in the receiver is given by

$$N = k T_o \cdot B_r \cdot F$$

Where

- k =Boltzmann's constant $1.38 \cdot 10^{-33} (J/^\circ k)$;
- T_o =noise temperature- $290^\circ K$;
- B_r =noise bandwidth, $Hz = 1/r$;
- F =noise factor;
- r =radar pulse width, sec.

The signal to noise ratio from (4.23) is

$$S/N = \frac{P_T G_T G_R \alpha \lambda^2}{(4\pi)^3 R^4 L_R K T_o B_r F} \quad (4.24)$$

The maximum radar range can be obtained by manipulating (4.24) as [13]

$$R_{\max} = \left[\frac{P_T G_T G_R \alpha \lambda^2}{(4\pi)^3 (S/N)_{\min} L_R K T_o F B_R} \right]^{\frac{1}{4}} \quad (4.25)$$

Where $(S/N)_{\min}$ is the single-pulse signal-to-noise ratio

Now consider a noise jammer with power

$$P_j = p_j B_j \quad (4.26)$$

Where

p_j = jammer power density, W/Hz

B_j = jammer bandwidth, Hz

The jammer power density at the radar receiver is given by

$$P_{jr} = \frac{p_j G_j G_{sl} \lambda^2}{(4\pi)^2 R_j^2 L_j} \quad (4.27)$$

Where

G_j = jammer antenna gain, dB

G_{sl} = receiver antenna gain toward jammer, dB

R_j = rang between jammer and radar, m

L_j = jammer system losses

If we make the assumption that the jammer density is much greater than the noise power density (i.e., $p_{ji} \gg K T_o F$), then

$$R_{\max} = \left[\frac{P_T G_T G_R \alpha \lambda^2}{(4\pi)^3 (S/J)_{\min} L_R p_{jr} B_R} \right]^{\frac{1}{4}} \quad (4.28)$$

Where $(S/J)_{\min}$ is the signal-to-jamming ratio for the appropriate target and detection statistics, Substituting (4.27) and (4.26) into (4.28) result in

$$R_{\max} = \left[\frac{P_T G_T R_j^2 G_R B_j \alpha L_j}{4\pi (S/J)_{\min} P_j L_R G_j G_{sl} B_R} \right]^{\frac{1}{4}} \quad (4.29)$$

Equation (4.29) is appropriate for stand-off (or stand-in) jamming calculations, R_{\max} is often called the “burn through range” and indicates the range at which the radar overcomes the jamming effect. Note that the term (G_R/G_{sl}) represents the ratio between the peak antenna gain and the side-lobe level. For self-screening jamming, (4.29) can be simplified by letting $R_j = R_{\max}$ and $G_{sl} = G_R$, result in [14, 8]

$$R_{\max} = \left[\frac{P_T G_T}{4\pi \left(\frac{S}{J}\right)_{\min}} \cdot \frac{\alpha}{P_j G_j} \cdot \frac{B_j}{B_r} \cdot \frac{L_j}{L_R} \right]^{\frac{1}{2}} \quad (4.30)$$

Equation (4.30) reveals several jamming principles. Firstly, the term $\left(\frac{\alpha}{P_j G_j} \right)$ can be consider a figure of merit for the jammer. For the same jamming effect, if the target RCS (α) is decreased, then the self-protection jammer EIRP is decreased in the same proportion. Eventually no jammer is required if the radar cross section is low enough. The term (B_j/B_r) represents the ratio between the jamming and radar bandwidths. If this term approaches a value of 1 to 5, then the jamming is considered spot jamming. If $B_j \gg B_R$, then barrage jamming is being used. It is to the advantage of the jammer (R_{\max} is minimum) to be in a spot jamming mode [14].

The same comment apply to (4.29) for stand-off jamming with the additional observations that when R_j is increased, which is the enemy missal attack range, greater than 60Km, the burn-through range is increased, making the less effective. Also, maximizing the ratio (G_R/G_{SL}) using ultra low side lobes increases the burn-through range, there by diluting the jamming effect.

4.2.2.1 Noise Jammer Effectiveness

There are several factors that cause the effectiveness of noise jammer to be less than their theoretical capability. One significant factor is the need for a noise jammer to accommodate victim systems with various polarizations.

The most obvious method of obtain a noise jammer signal is to pass band-limited Gaussian noise (e.g., receiver or thermal noise) through a high power amplifier [21]. This method of generating a jammer waveform is called direct noise amplification. The noise need not be generated as RF, but can be generated at base hand (its spectral density appropriately shaped by band limiting filters) and then heterodyned to RF where it is power amplified and radiated.

Based on information theory it is reasoned that white (uniform spectral density) Gaussian nose is the best noise jamming waveform .This follow because white Gaussian noise has the maximum entropy or uncertainty, of any random waveform for a specified average power. This conclusion is intuitively satisfying because it is statistically impossible to distinguish between receivers noise generated in the victim system and the externally jammer waveform.

4.3 Repeater Jamming Equation

In repeater mode, the signal enters the receiver antenna propagates through the RF preamplifier, through the RF switch, through the amplitude and the frequency or phase modulator, or through the power amplifier, and exits from the transmit antenna [4]. One of the most important factors to be considered in designing a repeater is the ratio of deception repeater signal level to the radar return as measured in the victim radar's receiver. The jam-to-signal ratio must be of the order of at least 7 dB to 10 dB to allow the jammer to capture the radar's tracking circuits [14]. This requirement translates into a repeater gain and power output specification.

To calculate the jam-to-signal ratio at the radar receiver, we will first develop expiration for the jammer signal. The transmitted radar signal received at the repeater jammer (P_{JR}) is given by [14]

$$P_{JR} = \frac{P_T G_T \lambda^2 G_{JR}}{(4\pi R)^2 L_p} \quad (4.31)$$

Where G_{JR} is the repeater jammer's receiving antenna gain, L_p is a loss term due to the possible use of different polarizations between the jammer and radar antennas and other

losses, and $P_T G_T$ is the radar's EIRP. The repeater jammer signal at the terminals (P_{RJ}) is then given by

$$P_{RJ} = \frac{P_T G_T^2 \lambda^4 G_{JR} G_{JT} G_e}{(4\pi R)^4 L_p^2} \quad (4.32)$$

Where G_{JT} is the repeater's transmitting antenna gain and G_e is the repeater's overall amplifiers gain minus any losses other than polarization that are experienced by the repeater jamming signal and not by the radar return signal. The signal returned to the radar is given by

$$P_R = \frac{P_T G_T^2 \lambda^2 \sigma}{(4\pi R)^3 R^4} \quad (4.33)$$

Where losses common, to the repeated jammer, signal are not explicitly shown. Then the jam-to-signal ratio is given by

$$\alpha = \frac{J}{S} = \frac{\lambda^2 G_{JR} G_{JT} G_e}{4\pi \sigma L_p^2} \quad (4.34)$$

, which is independent of range. Next, define $\sigma_e = \sigma \alpha$, which expresses the magnified radar cross section desired from the repeater and compute; the repeater gain as

$$G_{REP} = G_{JR} G_{JT} G_e = \frac{4\pi \sigma_e L_p^2}{\lambda^2} \quad (4.35)$$

, which is similar to the expiration for the capture area of an antenna. In addition, the repeater signal is sometimes commuted or gated at a high rate to prevent self-oscillation, which reduces the effective jammer signal average power. For a gated repeater with duty cycle $\beta \leq 1$ the repeater gain becomes

$$G_{REP} = \frac{4\pi \sigma_e L_p^2}{\lambda^2 \beta^2} \quad (4.36)$$

The power output of the repeater (P_J) can be found by multiplying (P_{RJ}) by the repeater's electronic gain

$$P_J = \frac{P_T G_T \lambda^2 G_{JR} G_e}{(4\pi R)^2 L_p} \quad (4.37)$$

From (4.36) the electronic gain is given by

$$G_e = \frac{4\pi\sigma_e L_p^2}{\lambda^2 G_{JR} G_{JT} \beta^2}$$

Substituting this into (4.37) results in an alternative expression for the jammer's output power [4,14]

$$P_J = \frac{P_T G_T L_p \sigma_e}{4\pi R^2 G_{JT} \beta^2} \quad (4.38)$$

4.4 Range Reduction Factor

Consider a radar system whose detection range R in the absence of jamming is governed by

$$(SNR)_o = \frac{P_i G^2 \lambda^2 \sigma}{(4\pi)^3 k T_e B_r FLR^4} \quad (4.39)$$

The term Range Reduction Factor (RRF) refers to the reduction in the radar detection range due to jamming. More precisely, in the presence of jamming the effective radar detection range is

$$R_{dj} = R \times RRF \quad (4.40)$$

In order to compute RRF, consider a radar characterized by Eq. (4.39), and a barrage jammer whose output power spectral density is J_0 (i.e., Gaussian like). Then the amount of jammer power in the radar receiver is

$$J = k.T_J.B_r \quad (4.41)$$

, where T_J is the jammer effective temperature. It follows that the total jammer plus noise power in the radar receiver is given by

$$N_i + J = k.T_e.B_r + k.T_J.B_r \quad (4.42)$$

In this case, the radar detection range is now limited by the receiver signal-to-noise plus interference ratio rather than SNR [24].

$$\left(\frac{S}{J + N} \right) = \frac{P_i G^2 \lambda^2 \sigma}{(4\pi)^3 k (T_e + T_J) B_r FLR^4} \quad (4.43)$$

4.5 The Effect of Swerling, Loss and UAV length for jamming analysis

Baron's and Alberhseim's methods are used to calculate the various detection factors associated with the Swerling target models.

For Doppler radar, the number of effective coherent pulses is calculated by the ratio of the PRF to the Doppler bandwidth. The numbers of non-coherent pulses are to be integrated is determined by dividing the total number of hits by the number of effective coherent pulses. For a non-Doppler radar, the non-Doppler bandwidth, is made equals to the radar's PRF so that all pulses are non-coherent integrated.

The jamming bandwidths (both self-screening and stand-off) must be adjusted so that they are larger than the frequency agility bandwidth of the radar. For target detection, the number of independent hits is calculated as $n_e = 1 + 2\Delta f l / c \leq n$ where l is the target length (Note: in this study the radar target are various types of fighter air craft including UAV which has 8.2 m length) and Δf is the frequency agility bandwidth [14].

The relationship used to find the jamming range is

$$R_j = \frac{R_c}{\left[1 + \frac{1}{L_a} \left(\frac{R_o}{R_{sso}}\right) + \sum_{i=1}^n \left(\frac{R_o}{R_{ssoi}}\right)^4\right]^{1/4}} \quad (4.44)$$

Where

$$R_c = R_o 10^{-Di(n)/40}$$

And R_o is the clear range where $S/N=1$

$$R_o = 129.2 \left[\frac{P_{t(KW)} G_t G_r \tau_{\mu s} \sigma}{f^2 (MHz) T_s L_R} \right]^{1/4} \quad (4.45)$$

R_{sso} is the range with **self-screening jamming** and $S/J=1$

$$R_{sso} = 4.8116 \times 10^{-3} \left[\frac{P_{t(KW)} G_t G_r \tau_{\mu s} \sigma}{P_{j(W/MHz)} G_j L_j} \right]^{1/2} \quad (4.46)$$

And R_{ssoi} is the range for each individual **stand-off jammer**

$$R_{ssoi} = \left(R_j R_{ssoi}^* \right)^{1/2} \left(\frac{G_R}{G_{Ri}} \right)^{1/4} \quad (4.47)$$

Where

$R_{ssoi}^* = R_{ssoi}$ evaluated at $P_j G_j L_j$ for the stand-off jammer

P_j = Jammer noise spectral density (W/Hz)

G_j = Jammer antenna gain

G_{Rj} = Radar antenna gain in direction of jammer

R_j = Range between the radar and jammer

L_j = jammer loss

$D_i(n)$ = The appropriate delectability factor in decibels for the appropriate Swerling type P_d , P_{fa} , and the number (n) of integral pulses

The loss term due to atmospheric and rain attenuation is

$$La = 10^{L_{db}/20} \quad (4.48)$$

Where

$$L_{dB} = K_a R_E (1 - e^{-R/R_E}) + r k_{aR} R$$

K_a = Standard atmospheric coefficient (dB/Km)

K_{aR} = Weather coefficient (dB/Km)

r = Rain rate (mm/hr)

R_E = Range parameter calculated from ϕ_c

$$\phi_c = \phi_t + \frac{2.5 \times 10^{-4}}{\phi_t + 0.028}$$

, where ϕ_t is the target's elevation angle. The range parameter in kilometres is then

$$R_E = \frac{3}{\sin(\phi_c)}$$

, where the preceding relationship uses an approximation

The range equation is

$$F(R) = \log(R_j / R_c) + \frac{1}{4} \log(1 + a / La + b) = 0 \quad (4.49)$$

$$a = \left(\frac{R_0}{R_{ss0}}\right)^4 \quad b = \left(\frac{R_0}{R_{soo}}\right)^4$$

The derivative is

$$F'(R) = (1/R) - \frac{aL'a}{4L^2a(1+b) + aLa}$$

Where

$$L'a = 2.303La \left[\frac{1}{R} + \frac{K_{aR}}{20} + \frac{Ka}{20} e^{-R/R_E} \right]$$

The range found from

$$R_N = R_{N-1} - \frac{F(R_{N-1})}{F'(R_{N-1})} \quad \text{with starting value of} \quad (4.50)$$

$$R_{N-1} = R_{ss0} \text{ , for **self-screening jamming** and}$$

$$R_{N-1} = R_{soo} \text{ , for **stand-off jamming** .}$$

4.6 Jammer Transmitting and Receiving Antennas

For jammer system directional antenna is more preferable so as to radiates greater power in specific directions allowing for increased performance on transmit and receive and reduced interference from unwanted sources.

4.6.1 Directivity, Gain, and Beam-width

The directive gain of an antenna system towards a given direction (θ, ϕ) is the radiation intensity normalized by the corresponding isotropic intensity, that is,[11,12].

$$D(\theta, \phi) = \frac{U(\theta, \phi)}{U_I} = \frac{U(\theta, \phi)}{P_{rad} / 4\pi} = \frac{4\pi}{P_{rad}} \frac{dP}{d\Omega} \quad (4.51)$$

Where $U(\theta, \phi)$ radiation intensity, P_{rad} power radiated, U_I isotropic radiation intensity. It measures the ability of the antenna to direct its power towards a given direction. The maximum value of the directive gain, D_{max} , is called the directivity of the antenna and will be realized towards some particular direction, say (θ_0, ϕ_0) . The radiation intensity will be maximum towards that direction, $U_{max} = U(\theta_0, \phi_0)$, so that

$$D_{\max} = \frac{U_{\max}}{U_i} \tag{4.52}$$

The directivity is often expressed in dB, Re-expressing the radiation intensity in terms of the directive gain, we have:

$$\frac{dP}{d\Omega} = U(\theta, \phi) = D(\theta, \phi)U_i = \frac{P_{\text{rad}} D(\theta, \phi)}{4\pi} \tag{4.53}$$

and for the power density in the direction of (θ, ϕ) :

$$\frac{dP}{dS} = \frac{dP}{r^2 d\Omega} = \frac{P_{\text{rad}} D(\theta, \phi)}{4\pi r^2}$$

where the power dP intercepting the area element $dS = r^2 d\Omega$ defines the power per unit area, or the power density of the radiation.

In the direction of maximum gain of the antenna, the quantity $P_{\text{rad}} \cdot D_{\max}$ will be referred as the effective isotropic radiated power (EIRP). It defines the maximum power density achieved by the antenna:

$$\left(\frac{dP}{dS}\right)_{\max} = \frac{P_{\text{EIRP}}}{4\pi r^2} \tag{4.54}$$

, where $P_{\text{EIRP}} = P_{\text{rad}} D_{\max}$

A related concept is that of the power gain, or simply the gain of an antenna. It is defined as in Eq. (4.51), but instead of being normalized by the total radiated power, it is normalized to the total power P_T accepted by the antenna terminals from a connected transmitter, as shown in Fig. 4.3

$$G(\theta, \phi) = \frac{U(\theta, \phi)}{P_T / 4\pi} = \frac{4\pi}{P_T} \frac{dP}{d\Omega} \tag{4.55}$$

Moreover, the power P_T may differ from the power radiated, P_{rad} , because of several loss mechanisms, such as ohmic losses of the currents flowing on the antenna wires or losses in the dielectric surrounding the antenna.

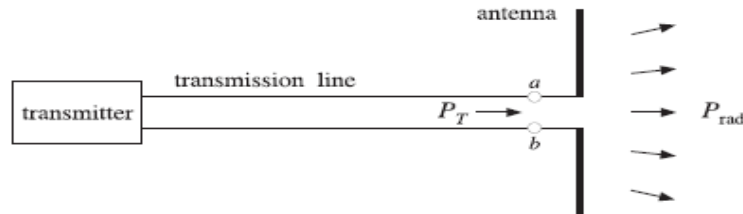


Fig. 4.3 Power delivered to an antenna versus power radiated

The definition of power gain does not include any reflection losses arising from improper matching of the transmission line to the antenna input impedance. The efficiency factor of the antenna is defined by:

$$e = \frac{P_{rad}}{P_T} \Rightarrow P_{rad} = eP_T \quad (4.56)$$

In general value of e is $0 \leq e \leq 1$. For a lossless antenna the efficiency factor will be unity and $P_{rad} = P_T$ (transmitted power). In such an ideal case, there is no distinction between directive and power gain.

$$G(\theta, \phi) = eD(\theta, \phi) \quad (4.57)$$

The maximum gain is related to the directivity by $G_{max} = e \cdot D_{max}$. It follows that the effective radiated power can be written as $P_{rad} \cdot D(\theta, \phi) = P_T G(\theta, \phi)$, and the

$$EIRP, P_{EIRP} = P_{rad} D_{max}$$

The angular distribution functions are defined so far are $G(\theta, \phi)$, $D(\theta, \phi)$, $U(\theta, \phi)$ which are all proportional to each other. Each of these brings out a different aspect of the radiating system.

In describing the angular distribution of radiation, it proves convenient to consider it relative to its maximal value. Thus, we define the normalized power pattern, or normalized gain by:

$$g(\theta, \phi) = \frac{G(\theta, \phi)}{G_{max}} \quad (4.58)$$

Because of the proportionality of the various angular functions, we have:

$$g(\theta, \phi) = \frac{G(\theta, \phi)}{G_{max}} = \frac{D(\theta, \phi)}{D_{max}} = \frac{U(\theta, \phi)}{U_{max}} \quad (4.59)$$

Writing $P_T G(\theta, \phi) = P_T \cdot G_{max} g(\theta, \phi)$, we have for the power density:

$$\frac{dP}{dS} = \frac{P_T G_{max}}{4\pi r^2} g(\theta, \phi) = \frac{P_{rad}}{4\pi r^2} g(\theta, \phi) \quad (4.60)$$

This form is useful for describing radar antenna. The normalized gain is usually displayed in a polar plot with polar coordinates (ρ, θ) such that $\rho = g(\theta)$, as shown in Fig.4.4 (this figure depicts the gain of a half-wave dipole antenna given by $g(\theta) = \cos^2(0.5\pi \cos \theta) / \sin^2 \theta$). The 3-dB, or half-power, beam-width is defined as the difference $\Delta\theta_B = \theta_2 - \theta_1$ of the 3-dB angles at which the normalized gain is equal to 1/2, or, -3 dB.

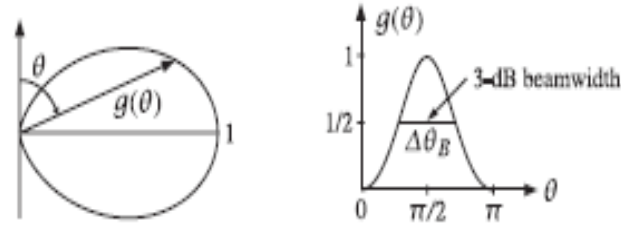


Fig. 4.4 Polar and regular plots of normalized gain versus angle

Another useful concept is that of the beam solid angle of an antenna. The definition is motivated by the case of a highly directive antenna, which concentrates all of its radiated power P_{rad} into a small solid angle $\Delta\Omega$, as illustrated in Fig.4.5

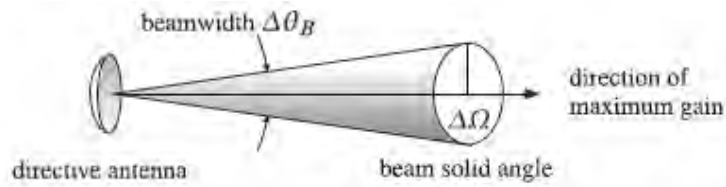


Fig. 4.5 Beam solid angle and beamwidth of a highly directive antenna

The radiation intensity in the direction of the solid angle will be:

$$U = \frac{\Delta P}{\Delta\Omega} = \frac{P_{rad}}{\Delta\Omega} \quad (4.61)$$

, where $\Delta P = P_{rad}$ by assumption. It follows that: $D_{max} = 4\pi U/P_{rad} = 4\pi/\Delta\Omega$, or,

$$D_{max} = \frac{4\pi}{\Delta\Omega} \quad (4.62)$$

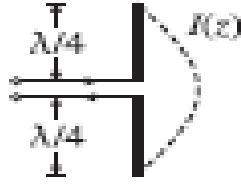
Antenna gain can be calculated by

$$G = 4\pi \frac{A_e}{\lambda^2}, \text{ where } A_e \text{ effective area of aperture, same unit as } \lambda^2 \text{ and less than one}$$

[36, 22]; by taking $A_e=0.5$ (average value) and at the radar operating frequency, the jammer antenna gain could be 12dB.

4.6.2 Half-Wave Dipole

The half-wave dipole corresponding to $l = \lambda/2$ or $L = 0.5$ is one of the most popular antennas. In this case, the current distribution along the antenna takes the form [12].



with $-\lambda/4 \leq z \leq \lambda/4$. The normalized gain is:

$$I(z) = I \cos(kz) \tag{4.63}$$

$$g(\theta) = \frac{\cos^2(0.5\pi \cos \theta)}{\sin^2 \theta} \tag{4.64}$$

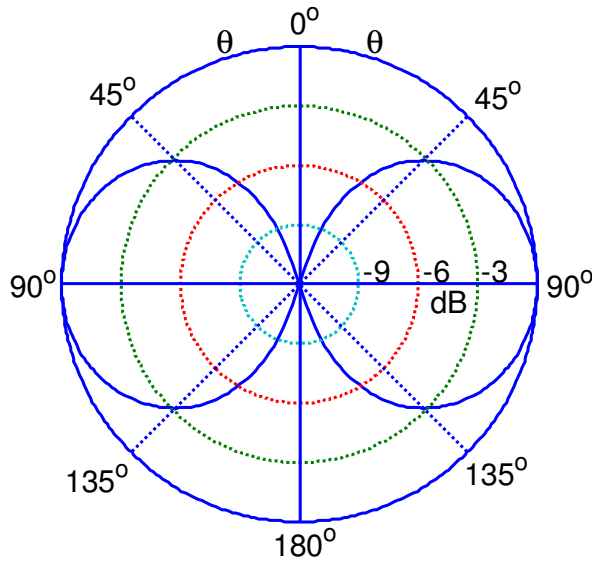


Fig. 4.6 Gain of half-wave dipole in dB units

Fig. 4.6 shows the gain in absolute and dB units. The 3-dB or half-power circle intersects the gain at an angle of $\theta_{3dB} = 44^\circ$, and a half-power beam width of $HPBW = 180^\circ - 2\theta_{3dB} = 92^\circ$.

The jammer beam solid angle can be evaluated numerically using MATLAB, and we find:

$$\Delta\Omega = 8.2666 \text{ The directivity is: } D_{\max} = \frac{4\pi}{\Delta\Omega} = 1.52 = 1.82 \text{ dB}$$

Using $P_{EIRP} = P_{\text{rad}} D_{\max}$, and Equation (4.24), $P_{\text{rad}}(\text{dB}) = (P_t + G_j - D_{\max} - L_j) \text{ dB} = 15.8 \text{ dB}$ (Note: the jammer loss in this case excluding the atmospheric, troposphere, rain fall and attenuation losses, since these losses are considered after radiation.)

The efficiency factor, using Eq. (4.56) and the above result, equals to 0.76.

Note: In order to get more directivity gain, the jammer system use reflector.

CHAPTER 5

DETECTION OF UAV-PLATFORM JAMMER

The noise additive to the received radar signal has Gaussian statistics is considered for ease of analysis. Fortunately, in general, nature is kind enough to provide receiver noise that is approximately Gaussian.

5.1 Properties of a Stationary Gaussian Noise

Consider a noise waveform $n(t)$ that is a sample function of a stationary Gaussian random process. A random variable \mathbf{n} is called Gaussian if its probability density function has the form of: [13, 19, 20]

$$p(n) = \frac{1}{\sqrt{2\pi\sigma_n^2}} e^{-\frac{(n-\langle n \rangle)^2}{2\sigma_n^2}} \quad (5.1)$$

Where $p(n)$ is independent of time and Mean-square deviation of noise, which is independent of time by virtue of the stationary property is

$$\sigma_n^2 = \langle [n - \langle n \rangle]^2 \rangle = \langle n^2 \rangle - \langle n \rangle^2 \quad (5.2)$$

$\langle n(t) \rangle = \langle n \rangle =$ Mean noise voltage, also independent of time

If the noise is ‘narrowband,’ and ‘zero mean,’ i.e., it can be expressed in the form

$$n(t) = x_n(t) \cos \omega_0 t + y_n(t) \sin \omega_0 t \quad (5.3)$$

Then

$$\langle x_n(t) \rangle = \langle y_n(t) \rangle = 0 \quad (5.4)$$

$$\langle x_n^2(t) \rangle = \langle x_n^2 \rangle = \langle y_n^2(t) \rangle = \langle y_n^2 \rangle = \langle n^2 \rangle = \sigma_n^2 \quad (5.5)$$

$$\langle x_n(t_1) y_n(t_2) \rangle = 0 \quad \text{for all } t_1, t_2 \quad (5.6)$$

The joint (bivariate) PDF of x_n and y_n is

$$p(x_n, y_n) = \frac{1}{\sqrt{2\pi\langle x_n^2 \rangle}} e^{-x_n^2 / 2\langle x_n^2 \rangle} \frac{1}{\sqrt{2\pi\langle y_n^2 \rangle}} e^{-y_n^2 / 2\langle y_n^2 \rangle} \quad (5.7)$$

$$= \frac{1}{2\pi\sigma_n^2} e^{-\frac{(x_n^2 + y_n^2)}{2\sigma_n^2}} \quad (5.8)$$

Where (5.4,5.5 and 5.6) must be invoked in deriving (5.7) from the general form of the bivariate Gaussian PDF, which involves the ACF(autocorrelation function) of x_n and y_n , all of which are set equal to zero in (5.7). The form (5.7) expresses $p(x_n, y_n)$ as the product of the p.d.fs' of x_n and y_n , i. e., assumes they are statistically independent. In the Gaussian case, (5.6) implies statistical independence, but in general, the two variables being uncorrelated do not necessarily correspond one-to-one with statistical independence.

If (5.4) does not apply, i. e, if $\langle x_n \rangle$ and $\langle y_n \rangle$ are nonzero, then the PDF of (5.7) can be generalized to the form of:

$$p(x, y) = \frac{1}{2\pi\sigma_n^2} e^{-[(x-\langle xn \rangle)^2 + (y-\langle yn \rangle)^2] / 2\sigma_n^2} \quad (5.9)$$

Where $x = x_n + \langle x_n \rangle$, $y = y_n + \langle y_n \rangle$.

Equations (5.1) and (5.9) can be used in the case of a nonzero signal plus noise voltage, where $\langle n \rangle = 0$ in (5.1), as implied by (5.3) and (5.4)

$$\begin{aligned} v(t) &= s(t) + n(t) = x(t) \cos \omega_0 t + y(t) \sin \omega_0 t \\ &= [x_s(t) + x_n(t)] \cos \omega_0 t + [y_s(t) + y_n(t)] \sin \omega_0 t \end{aligned} \quad (5.10)$$

5.2 Detection Probability and False Alarm Probability

The detection problem is that of determination of the presence of a signal within the noise. The “detection probability” P_d is the conditional probability that, given that a signal is present, the signal-plus-noise falls within the range that will result in a “signal present” decision. The false alarm probability (Pfa) is the conditional probability that, given that no signal is present the noise falls within a range that will result in a “signal present” decision, i.e., in the latter case, the detection criterion produces a false indication of signal presence, popularly known as a “false alarm.” [1, 10, 21, 31].

Mathematically, these quantities are given by

$$P_d = \int_{VT}^{\infty} dv p(v/s) \quad (5.1)$$

$$P_{fa} = \int_{V_T}^{\infty} dp \quad (v / n) \quad (5.12)$$

Where V_T is a chosen “threshold” voltage level, such that, if $v(t)$ falls above that threshold, the decision will be “radar signal present” and if $v(t)$ falls below the threshold, the decision will be “noise alone,” and where $p(v/s)$ and $p(v/n)$ are the conditional PDFs of v given the condition “radar signal present” and “noise alone,” respectively[23].

For Gaussian noise

$$Pd = \frac{1}{2}[1 - \text{erf}(\hat{V}_T - u)] \quad (5.13)$$

$$Pfa = \frac{1}{2}[1 - \text{erf}(\hat{V}_T)] \quad (5.14)$$

Where $\hat{V}_T = V_T / \sqrt{2\sigma_n} =$ threshold voltage normalized to $\sqrt{2}$ times the root mean square (r. m. s) noise level and $\sqrt{|R|} = |s| \sqrt{2\sigma_n} = 1 / \sqrt{2}(\text{voltageSNR})$.

$u = \pm \sqrt{|R|}$ and $\text{erf}(x) = 2 / \sqrt{\pi} \int_0^{\infty} dy e^{-y^2} =$ error function, which is available in tabulated form in many text books.

Considering that the radar signal is a sine waveform with amplitude A , then its power is $A^2/2$, $\text{SNR} = A^2/2\psi^2$ (single-pulse SNR) and $(V_T^2 / 2\psi^2) = \ln(1/P_{fa})$, then

Marcum define as P_d which equal to

$$P_D = \int_{V_T}^{\infty} \frac{r}{\psi^2} I_0 \left(\frac{r^A}{\psi^2} \right) \exp \left(-\frac{r^2 + A^2}{2\psi^2} \right) dr = Q \left[\sqrt{\frac{A^2}{\psi^2}}, \sqrt{2 \ln \left(\frac{1}{P_{fa}} \right)} \right] \quad (5.15)$$

$$\sqrt{2\psi^2 \ln(1/P_{fa})}$$

$$Q[\alpha, \beta] = \int_{\beta}^{\infty} \zeta I_0(\alpha\zeta) e^{-(\zeta^2 + \alpha^2)/2} d\zeta \quad (5.16)$$

Q is called Marcum’Q-function [23, 26, 30]. Many approximations for computing Eq. (5.16) can be found in the literatures. The very accurate approximation presented by North

$$P_d \approx 0.5 \operatorname{erfc} \left(\left(\sqrt{-\ln P_{fa}} - \sqrt{\operatorname{SNR} + 0.5} \right) \right) \quad (5.18)$$

Where the complementary error function is [19]:

$$\operatorname{Erfc}(z) = 1 - \frac{2}{\sqrt{\pi}} \int_0^z e^{-v^2} dv \quad (5.19)$$

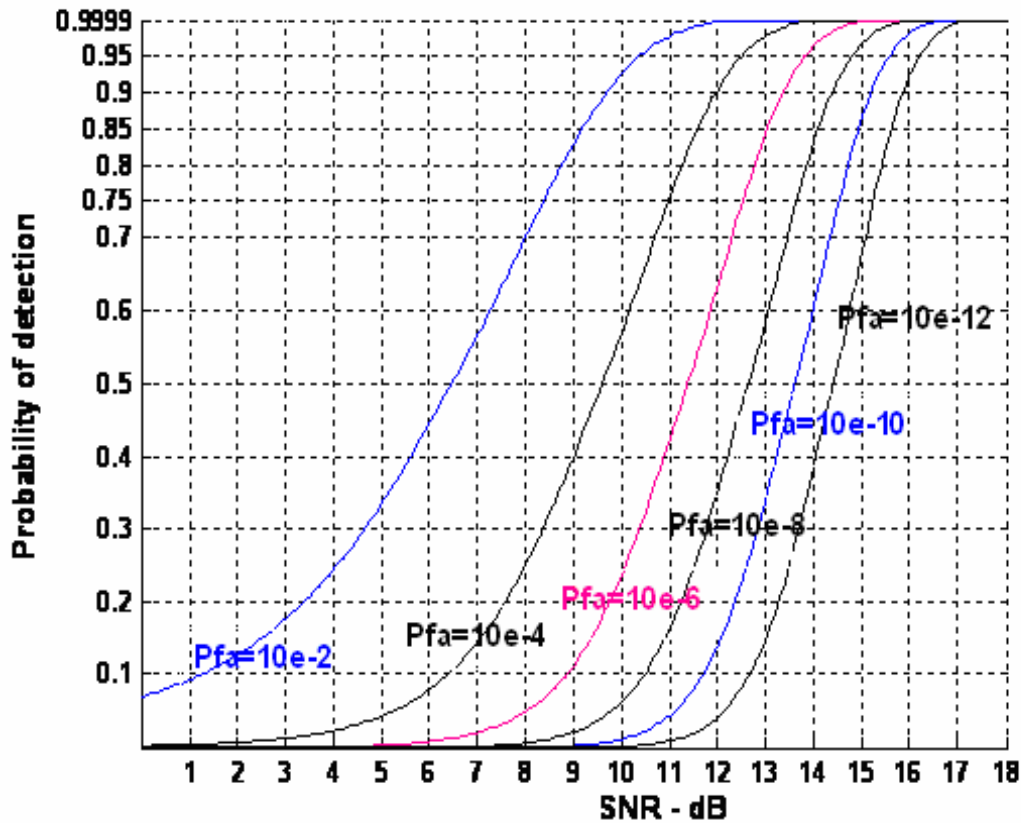


Figure 5.1 Probability of detection versus SNR, for several values of P_{fa} .

The sensitivity of the S/N required to the P_{fa} is illustrated in Fig.5.1, which is plotting Eq.5.16. This figure shows the S/N required to provide various values of P_d with P_{fa} as a parameter. The S/N required for detection increases moderately as P_{fa} decreases. Let us see a typical example, decreasing P_{fa} by two orders of magnitude from 10^{-6} to 10^{-4} , for $P_d=0.9$ requires increasing the S/N by only about 1.2 dB.

Since the jammer SNR = 12dB (see chapter 4) then the probability of detection and the corresponding probability false alarm of a jammer become as follows:

$$P_d=0.999 \text{ at } p_{fa}=10^{-2}, P_d=0.9 \text{ at } p_{fa}=10^{-4}, P_d=0.6 \text{ at } p_{fa}=10^{-6} \text{ and } P_d=0.35 \text{ at } p_{fa}=10^{-8}.$$

5.3 Pulse Integration

By adding all pulses transmitted by P-15 radar during a single scan, the jammer sensitivity (SNR) can be increased. The number of transmitted pulses depends on the antenna scan rate and the jammer PRF.

The process of adding jammer transmits from many pulses is called jammer pulse integration. Pulse integration can be performed on the quadrature comments prior to the envelope detector. This is called coherent integration or pre-detection integration. Coherent integration preserves the phase relationship between the received pulses. Thus a growth in the signal amplitudes is achieved. Alternatively, pulse integration performed after the envelope detector (where the phase relation is destroyed) is called non-coherent or post-detection integration [22].

5.3.1 Coherent Integration

In coherent integration, when a perfect integration is used (100% efficiency), to integrate n_p pulses the SNR is improved by the same factor. Otherwise, integration loss occurs, which is always the case for non-coherent integration. Coherent integration loss occurs when the integration process is not optimum. This could be due to received signal fluctuation, instability in the jammer local oscillator, or propagation path changes.

Consider the received signal, which has the sum of transmitted signal plus the random noise, [6], the m^{th} pulse is

$$y_m(t) = s(t) + n_m(t) \quad (5.20)$$

Where $s(t)$ is the radar transmits of interest and $n_m(t)$ is white uncorrelated additive noise signal. Coherent integration of n_p pulses yields

$$z(t) = \frac{1}{n_p} \sum_{m=1}^{n_p} y_m(t) = \sum_{m=1}^{n_p} \frac{1}{n_p} [s(t) + n_m(t)] = s(t) + \sum_{m=1}^{n_p} \frac{1}{n_p} n_m(t) \quad (5.21)$$

The total noise power in $z(t)$ is equal to the variance. More precisely,

$$\psi_{nz}^2 = E \left[\left(\sum_{m=1}^{n_p} \frac{1}{n_p} n_m(t) \right) \left(\sum_{l=1}^{n_p} \frac{1}{n_p} n_l(t) \right) \right] \quad (5.22)$$

Where $E[.]$ is the expected value operator. It follows that

$$\psi_{nz}^2 = \frac{1}{n_p^2} \sum_{m,l=1}^{np} E[nm(t)nl^*(t)] = \frac{1}{n_p^2} \sum_{m,l=1}^{np} \psi_{ny}^2 \delta_{ml} = \frac{1}{n_p} \psi_{ny}^2 \quad (5.23)$$

Where ψ_{nz}^2 is the single pulse noise power and δ_{ml} is equal to zero for $m \neq l$ and unity for $m = l$. Observation of Eqs. (5.21) and (5.23) shows that the desired signal power after coherent integrations unchanged, while the noise power is reduced by the factor $1/n_p$. Thus, the SNR after coherent integration is improved by n_p .

Denote the single pulse SNR required to produce a given probability of detection as $(SNR)_1$. Also, denote $(SNR)n_p$ as the SNR required to produce the same probability of detection when n_p pulses are integrated. It follows that [13, 22, 25, 31]

$$(SNR)n_p = \frac{1}{n_p} (SNR)_1 \quad (5.24)$$

5.3.2 Non-Coherent Integration

Non-coherent integration that are deigned to operate without knowledge of the incoming signal's phase, there for phase estimation is not required.

Non-coherent integration is often implemented after the envelope detector, also known as the quadratic detector. A block diagram of jammer receiver utilizing a square law detector and non-coherent integration is illustrated in Fig.5.2. In practice, the square law detector is normally used as an approximation to the optimum receiver.

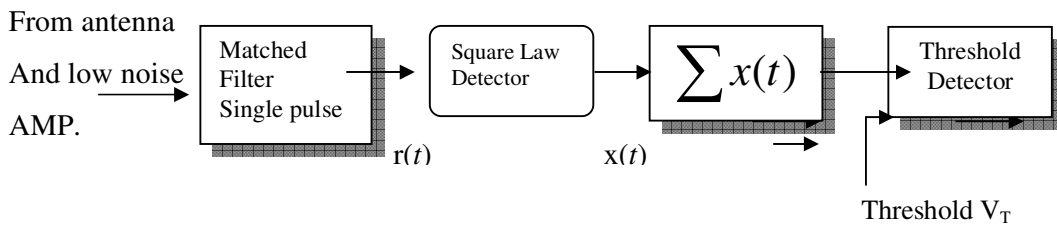


Figure 5.2 Simplified block diagram of a square law detector and non-coherent integration.

The Pdf for the signal $r(t)$ define a new dimensionless variable y as

$$yn = \frac{r_n}{\psi} \quad (5.25)$$

And also define

$$\mathfrak{R}_p = \frac{A^2}{\psi_2} = 2SNR \quad (5.26)$$

It follows that the .P df for the new variable is then given by

$$f(y_n) = f(r_n) \left| \frac{dr_n}{dy_n} \right| = y_n I_0(y_n \sqrt{\mathfrak{R}_p}) \exp\left(\frac{-(y_n^2 + \mathfrak{R}_p)}{2}\right) \quad (5.27)$$

The output of a square law detector for the n^{th} pulse is proportional to the square of its input, which, after the change of variable in Eq. (5.25), is proportional to y_n . Thus, it is convenient to define a new change variable,

$$x_n = \frac{1}{2} y_n^2 \quad (5.28)$$

The P_{df} for the variable at the output of the square law detector is given by

$$f(x_n) = f(y_n) \left| \frac{dy_n}{dx_n} \right| = \exp\left(-\left(x_n + \frac{\mathfrak{R}_p}{2}\right)\right) I_0(\sqrt{2x_n \mathfrak{R}_p}) \quad (5.29)$$

Non-coherent integration of n_p pulses is implemented as

$$z = \sum_{n=1}^{n_p} x_n \quad (5.30)$$

Since the random variables x_n are independent, the pdf for the variable z is

$$f(z) = f(x_1) \bullet f(x_2) \bullet \dots \bullet f(x_{n_p}) \quad (5.31)$$

The operator \bullet symbolically indicates convolution [19]. The characteristic functions for the individual pdfs can then be used to compute the joint pdf in Eq. (5.31). The detail of this development is not included in this study. The result is

$$f(z) = \left(\frac{2z}{n_p \mathfrak{R}_p}\right)^{(n_p-1)/2} \exp\left(-z - \frac{1}{2} n_p \mathfrak{R}_p\right) I_{n_p-1}(\sqrt{2n_p z \mathfrak{R}_p}) \quad (5.32)$$

I_{n_p-1} is the modified Bessel function of order n_p-1 . Therefore, the probability of detection is obtained by integrating $f(z)$ from the threshold value to infinity. Alternatively, the probability of false alarm is obtained by letting \mathfrak{R}_p be zero and integrating the Pdf from the threshold value to infinity. Closed form solutions to these integrals are not easily available. Therefore, numerical techniques are often utilized to generate tables for the probability of detection [6, 13, and 25].

5.4 Improvement Factor and Integration Loss

Denote the SNR that is required to achieve a specific P_d given a particular P_{fa} when n_p pulses are integrated non-coherently by $(SNR)_{NCI}$. And thus, the single pulse SNR, $(SNR)_1$, is less than $(SNR)_{NCI}$. More precisely,

$$(SNR)_{NCI} = (SNR)_1 \times I(n_p) \quad (5.33)$$

Where $I(n_p)$ is called the integration improvement factor. An empirically derived expression for the improvement factor that is accurate within 0.8 dB is reported Peebles as:

$$[I(n_p)]_{dB} = 6.79(1 + 0.235 P_D) \left(1 + \frac{\log(1/P_{fa})}{46.6} \log(n_p)\right) + (1 - 0.1401 \log(n_p) + 0.018310 (\log(n_p))^2) \quad (5.34)$$

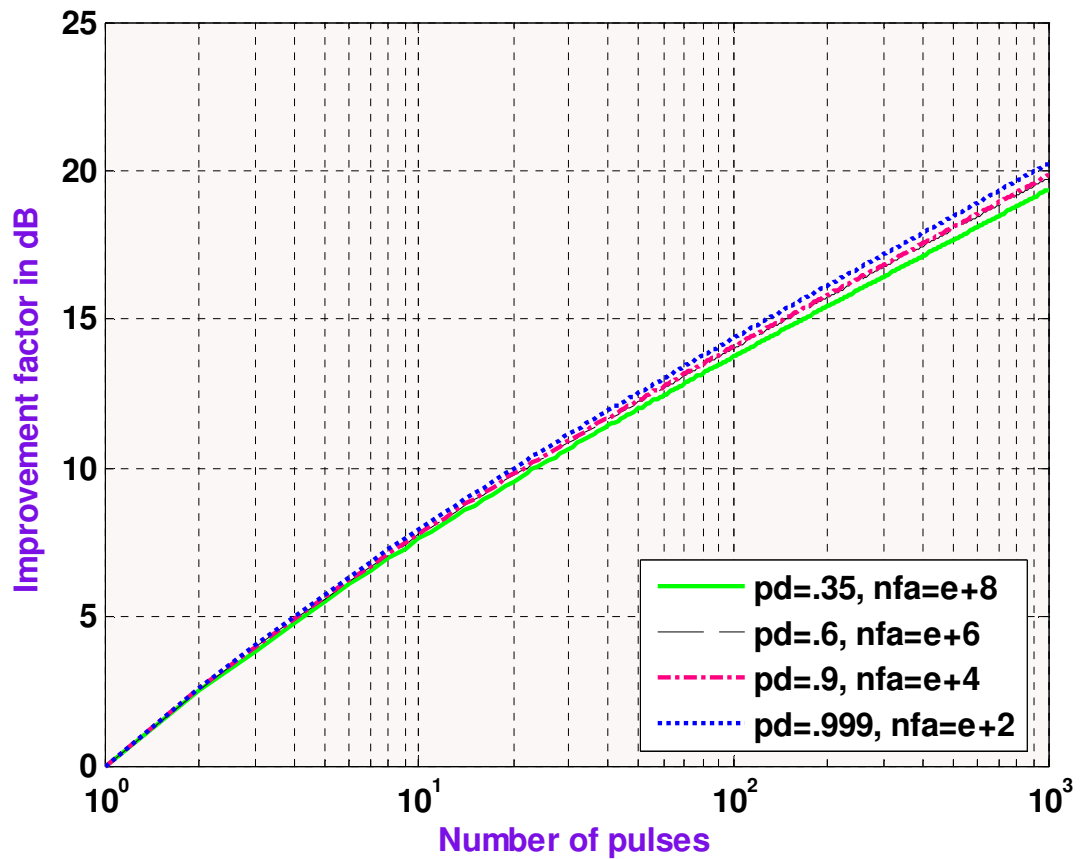


Figure 5.3 Integration- Improvement facto versus number of non-coherently integrated pulse

Fig. 5.3 shows plots of the integration improvement factor as a function of the number of integrated pulses and as parameters, actually the parameter can select in Figure 5.1. As the number of pulse increase the improvement factor also increase according to the probability of detection. For this thesis $n_p=10$ is selected and probability of detection $p_d=0.9$. If we increase the number of pulses the integration loss also increases, this effect can be clearly described the Figure 5.4. The signal to noise ratio will always than that of the pre-detection integrator for reasonable value of P_d [2,32].

The integration loss and the integration improvement factor are vary only slightly with probability of false alarm. In Figure 5.4 at $n_p=10$ and $P_d=0.9$ the integration jammer loss equal to 2.2dB.

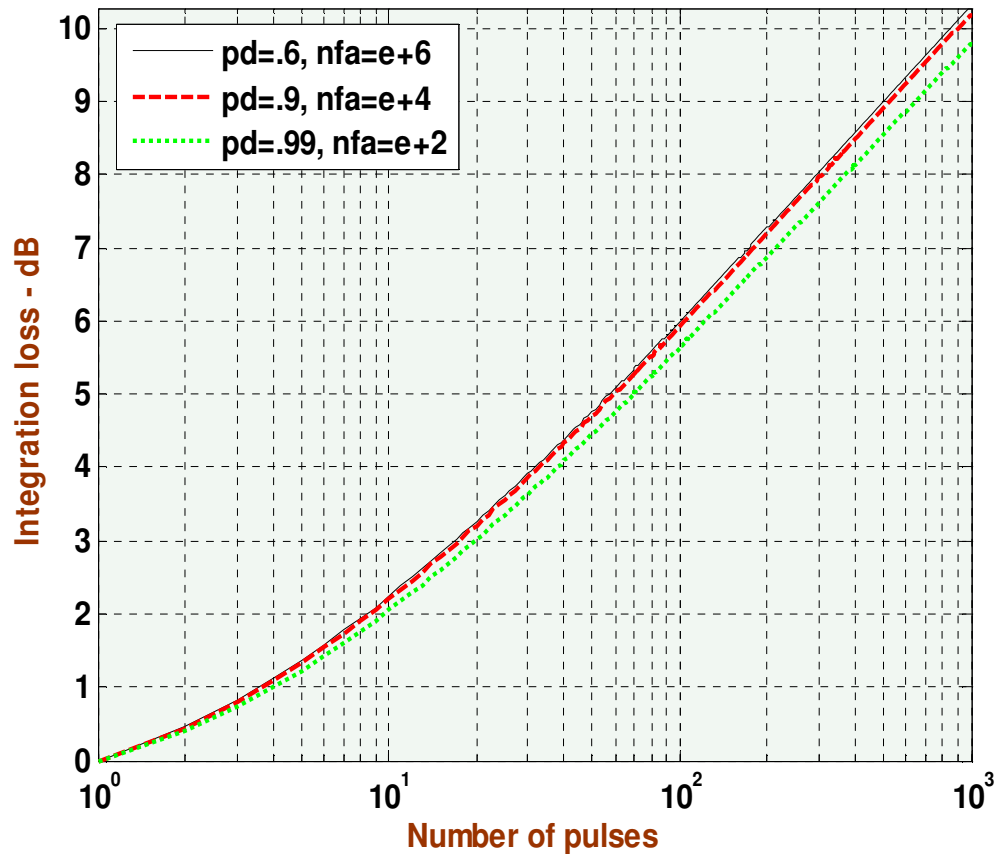


Figure 5.4 *Integration losses versus number of non-coherently integrated pulses*

5.5 Detection of Fluctuating Targets

Basically received signals are vary in amplitudes either in power or cross-sectional terms. These amplitudes can vary from scan to scan or between echo to echo due to aspect changes relative the receiver. This variation is often referred as target scintillation [1].

So far the probability of detection calculations assumed a constant RCS (non-fluctuating signal). This work was first analyzed by Marcum; Swirling 1 extended Marcum's work to four distinct cases that account for variations in the target cross section. These cases have come to be known as Swerling models. They are: Swerling I, Swerling II, Swerling III, and Swerling IV [13]. The constant RCS case analyzed by Marcum is widely known as Swerling 0 or equivalently Swerling V; the detail can be seen later. Signal fluctuation lowers the probability of detection, or equivalently reduces the SNR [1, 25].

This fluctuation is more important for radar receiver than the jammer receiver.

5.6 Threshold Selection

A threshold is “a value of voltage or other measure that a signal must exceed in order to be detected or retained for further processing” [25].

In jammer detection process, the received signal amplitude is compared with a threshold level. The threshold is usually set to exclude most noise signal. When the signal exceeds the threshold target detection is declared.

For uniformity, the more general gamma distribution is used for calculations. The power of Rayleigh noise is distributed according to the negative exponential distribution. This distribution is a gamma distribution with $N = 1$, namely,

$$P(Y) = \exp(-Y) \quad (5.35)$$

The distribution of the sum of N samples of noise taken from the same distribution is a gamma distribution with N degree is freedom.

$$P(Y) = \frac{Y^{N-1} \exp(-Y)}{(N-1)!} \quad (5.36)$$

There is a special case for one pulse, which has a negative exponential probability distribution, namely,

$$P(Y) = \exp(-Y) \quad (5.37)$$

If the noise is applied to a threshold Y_{fa} may be rewritten as:

$$P_{fa} = \int_{Y_b}^{\infty} \frac{Y^{N-1} \exp(-Y)}{(N-1)!} dY \quad (5.38)$$

The probability of a false alarm, P_{fa} may be rewritten as:

$$1 - P_{fa} = \int_0^{Y_b} \frac{Y^{N-1} \exp(-Y)}{(N-1)!} dY \quad (5.39)$$

For one noise sample, the probability of a false alarm is [18]

$$P_{fa}(1) = \exp(-Y_b) \quad (5.40)$$

Equation (5.39) is normally solved numerically. The limits for the solution can be found using Johnson’s approximation, which in itself is reasonably accurate, namely

$$Y_b = N - \sqrt{N} + 2.3\sqrt{+\log_{10} p_{fa}} \left(\sqrt{+\log_{10} p_{fa}} + \sqrt{N} - 1 \right) \quad (5.41)$$

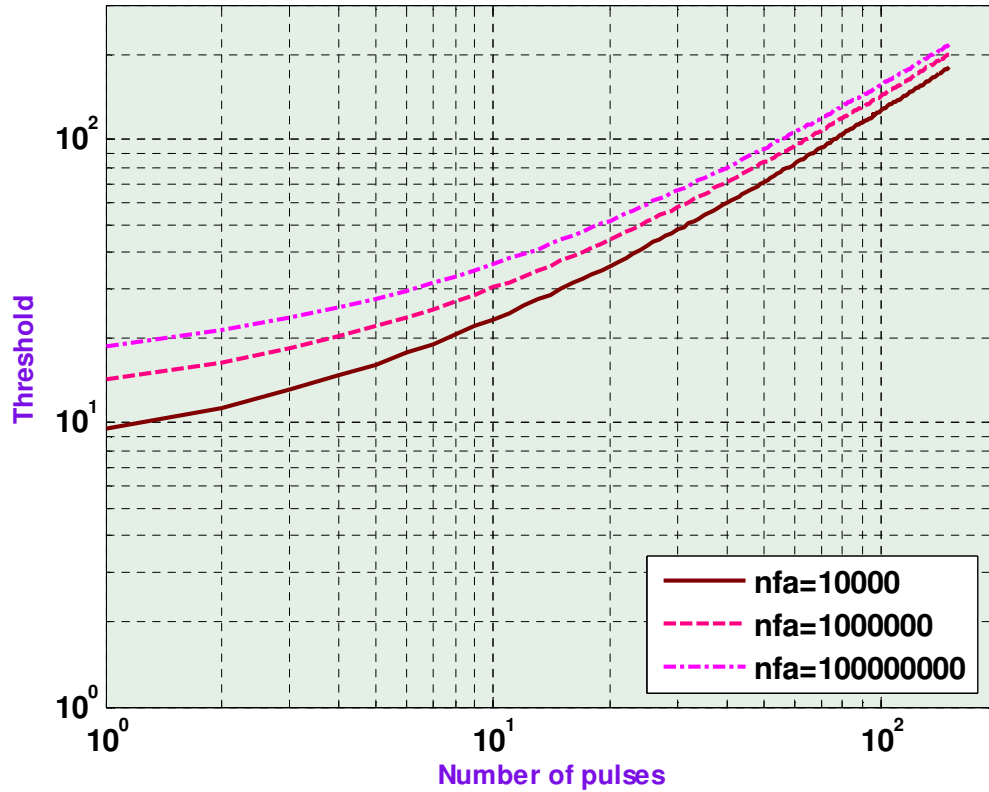


Figure 5.5 Threshold VT versus n_p for several values of nfa

When the false alarm number (inverse of the false-alarm probability) increase, the threshold values also increases as the parameter of number of pulse, at particular case, where $N_p=10$, $P_{fa}=10e-4$ and $P_d=0.9$ the threshold value becomes 50.This can be seen Figure (5.5), the curve plotted using equation(5.41).

5.7 Probability of Detection (For fluctuations Target)

Having discussed the probability of a false alarm caused by noise, the size of a signal plus noise sample required for detection is estimated [1,2].

5.7.1 Marcum case: no fluctuation

The no fluctuating, or Marcum case, sometimes called Swerling case 0 or 5, is for echoes from symmetrical objects, such as spheres, which have the same reflecting area in all directions. The probability distribution of signal plus noise is a Ricean [30] distribution and is given by

$$P(Y) = \left(\frac{Y}{RN}\right)^{\frac{N-1}{2}} \exp(-Y - NR) I_{N-1}(\sqrt{4NRY}) \quad (5.42)$$

, where $I_p(x)$ is the modified Bessel function of the first kind of order p .

The probability of detection, or the probability that the sum of signal plus noise exceeds the threshold, is the integral of (5.42) to the right of the threshold [1,18].

$$\begin{aligned} P_d &= \int_{y_b}^{\infty} \left(\frac{Y}{NR}\right)^{\frac{N-1}{2}} \exp(-Y - NR) I_{N-1}(\sqrt{4NRY}) dY \\ &= 1 - \int_0^{y_b} \left(\frac{Y}{NR}\right)^{\frac{N-1}{2}} \exp(-Y - NR) I_{N-1}(\sqrt{4NRY}) dY \end{aligned} \quad (5.43)$$

Approximate value for large numbers of hits may be

$$P_d = 1 - \int_0^{y_b} \frac{1}{\sqrt{2\pi N(1+2R)}} \exp\left(-\frac{[Y - N(1+R)]^2}{2N(1+2R)}\right) dY \quad (5.44)$$

, where R is the power signal-to-noise ratio.

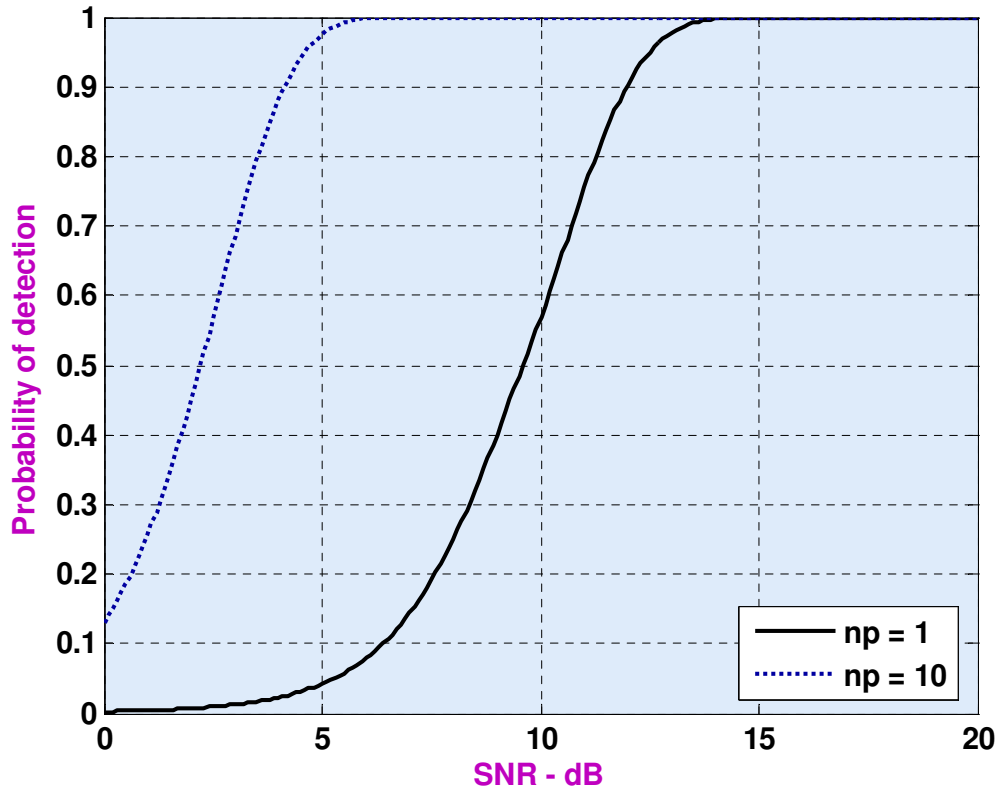


Figure 5.6 Probability of detection versus SNR, $Pfa=10e-4$, and non-coherent integration

It requires less SNR, with ten pulses integrated non-coherently, to achieve the same probability of detection as in the case of a single pulse. Hence, for any given P_D the SNR improvement can be read from the plot Figure 5.7.

5.7.2 Swerling case I: slow fluctuation

Swerling case I is the case for most rotating, fixed frequency air surveillance radars, which is fluctuation is slow. Aircraft are illuminated by a number of pulses for a short time during each antenna revolution or scan. The illumination time is taken to be too short for the aircraft to change its aspect during this time, so that the returning echoes have the same amplitude. The amplitude of the echoes is taken from a Raleigh voltage distribution or negative exponential power distribution corresponding to objects that have a large number of equal small reflectors. The probability distribution function for signal plus noise is given by [1, 13, 18]:

$$p(Y) = \frac{Y^{N-2}}{(N-2)!} - (1+NR) \frac{dp(Y)}{dY}$$

$$= \left(1 + \frac{1}{NR}\right)^{N-2} \exp\left(-\frac{Y}{1+NR}\right) Y \left(\frac{Y}{1 + \frac{1}{NR}}, N-1\right) \quad (5.45)$$

For more than one pulse, the signal plus noise distribution must be found to find the probability of detection

$$P_d = 1 - Y(N-1, Y) + \left(1 + \frac{1}{NR}\right)^{(N-1)} \exp\left(-\frac{Y}{1+NR}\right) Y \left(N-1, \frac{Y}{1 + \frac{1}{NR}}\right) \quad (5.46)$$

, where $y(a, x) = \int_0^x \exp(-t) t^{a-1} dt$.

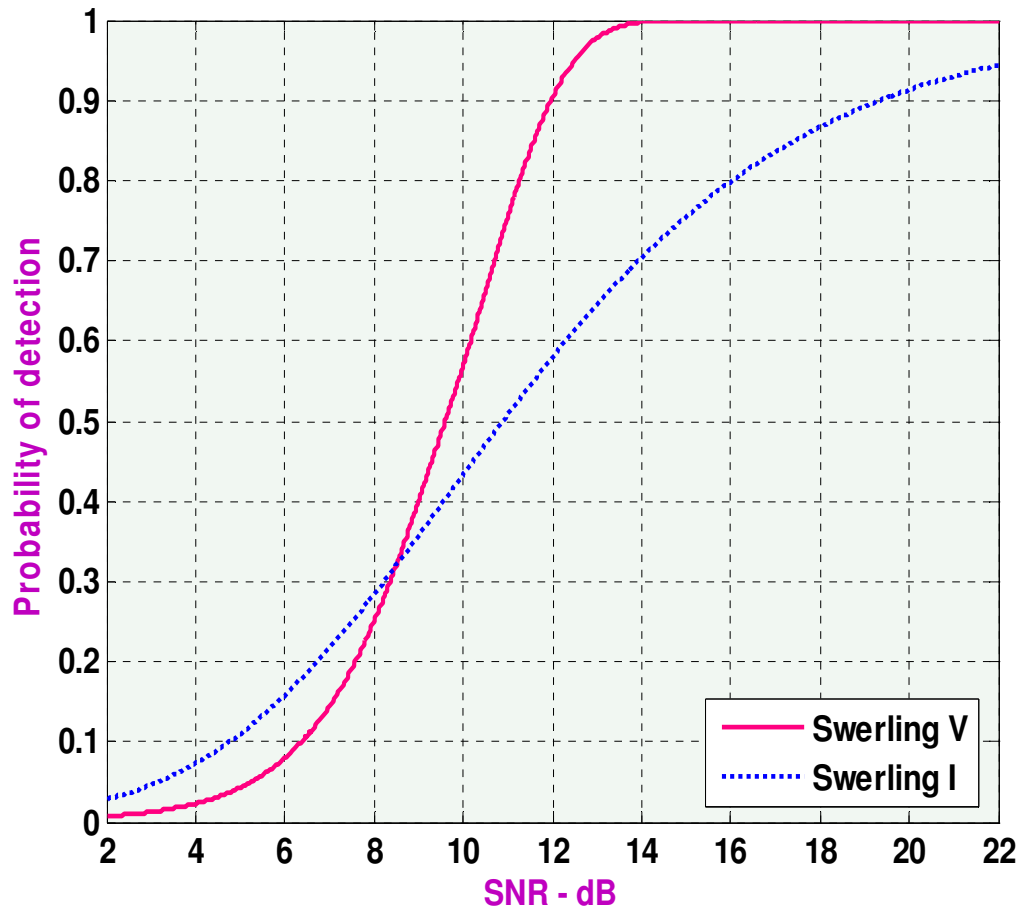


Figure 5.7 Probability of detection versus SNR, single pulse, $P_{fa}=10^{-4}$

Figure 5.7 plot shows that the S/N required for detection increase with increasing target signal fluctuation for values of Pd greater than above 0.32. This is because the signal must exceed the threshold.

The opposite effect occurs for values of S/N below about 0.32, since the fluctuation increase the probability of exceeds the threshold in this region.

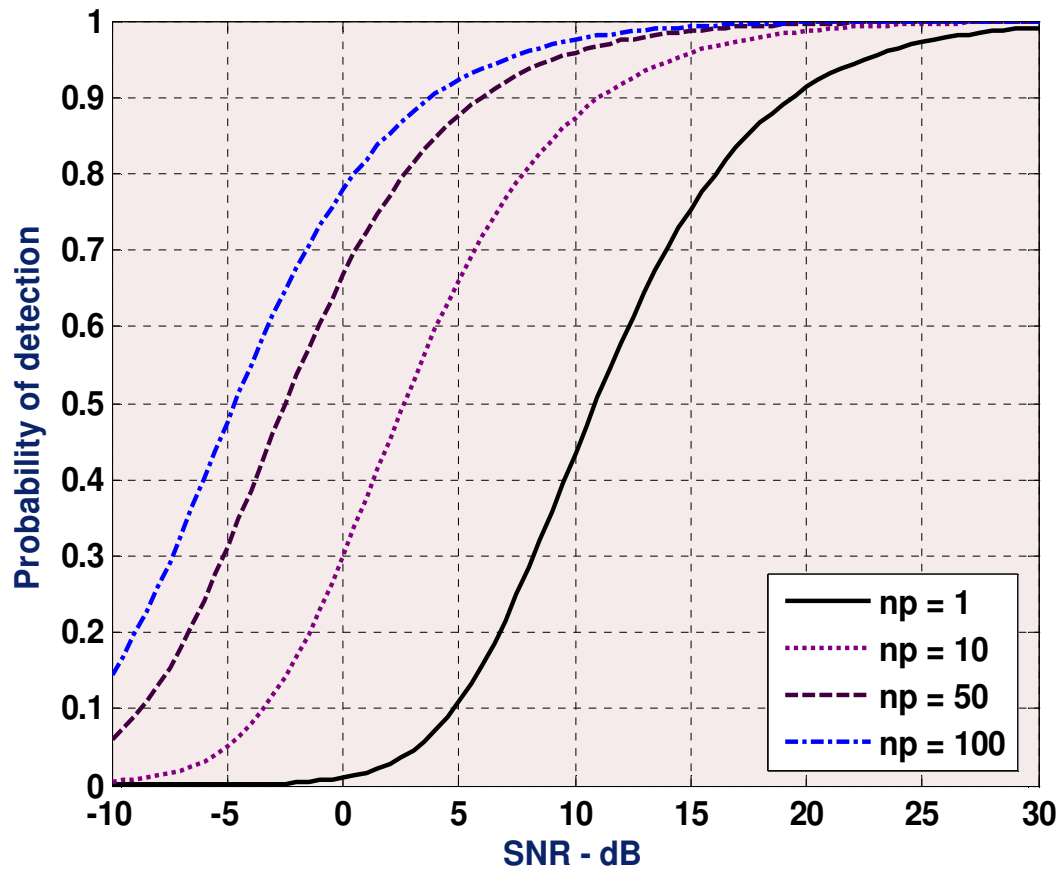


Figure 5.8 Probability of detection versus SNR. Swerling I $P_{fa}=10^{-4}$

5.7.3 Swerling case II: fast fluctuation

Swerling case II covers the case when the returning echoes are independent samples from a Rayleigh distribution, which happens with radars which change their transmitter frequency significantly from pulse to pulse (also called frequency agile radars). Each returning echo is the sum of the echoes from each small reflector, as in Swerling case 1. However a target becomes fast fluctuation.

The probability distribution of the sum of the received signals is that for the sum of N independent samples or a gamma distribution [26]. The received signals are generally many times larger than the noise echoes.

The probability distribution function of the gamma distributed signal sum plus gamma distributed noise sum depends on the signal – to – noise ratio. It is given by

$$p(Y) = \frac{1}{(1+R)^N} \frac{1}{(N-1)} Y^{N-1} \exp\left(-\frac{Y}{1+R}\right) \quad (5.47)$$

The false alarm probability gives the threshold Y The probability of detection of detection is

given by [1, 18] $P_d = 1 - y\left(N, \frac{Y_b}{1+R}\right)$ (5.48)

Where $y(a, x) = \int_0^x \exp(-t) t^{a-1} dt$.

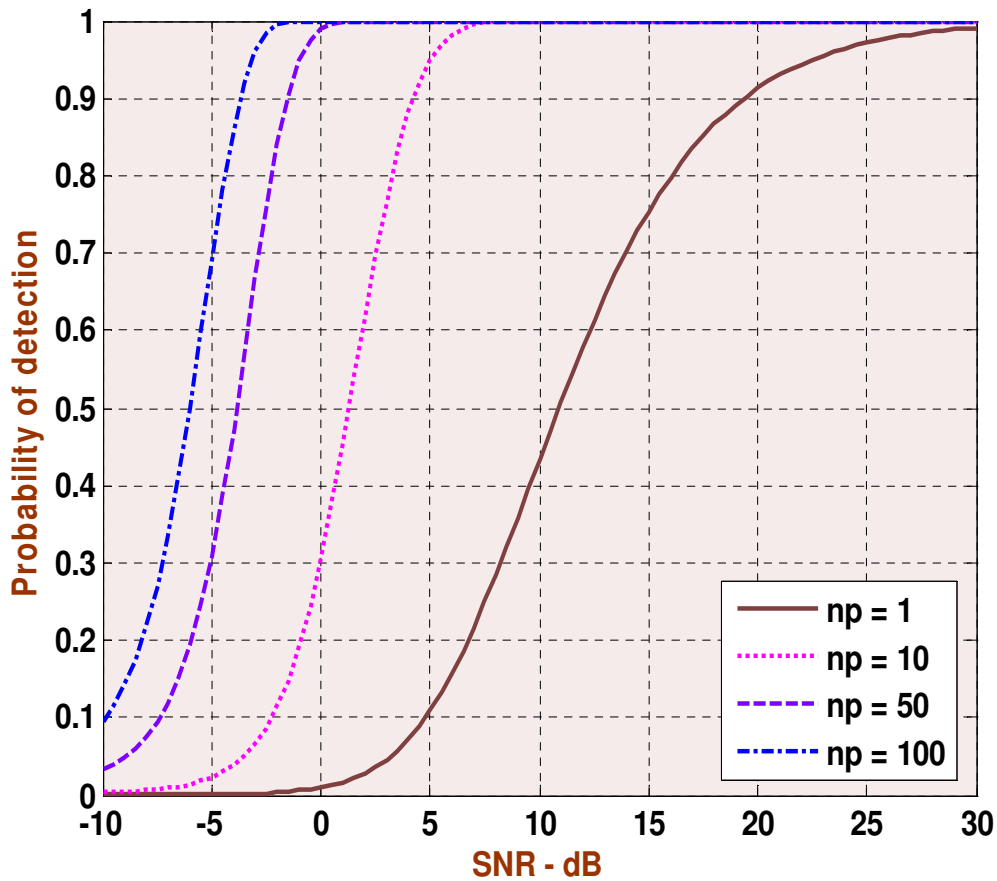


Figure 5.9 Probability of detection versus SNR. Swerling II $P_{fa}=10^{-4}$

5.7.4 Swerling case III: slow chi-squared fluctuation

Swerling case III and IV are similar to cases I and II, but the object of interest has one major reflector and many minor ones. The echoes have a chi-squared probability distribution function with four degrees of freedom Swerling case III echoes have the same amplitude during a look and different amplitudes from look (scan) to look. The probability distribution function for signal plus noise is given by

$$P(Y) = \frac{Y^{N-1} \exp(-Y)}{\left(1 + \frac{NR}{2}\right)^{N-1}} {}_1F_1\left(2, N; \frac{Y}{1 + \frac{2}{NR}}\right) \quad (5.49)$$

Where ${}_1F_1$ is the confluent hyper geometric function given by

$${}_1F_1(a; b; z) = \frac{\Gamma(b)}{\Gamma(b-a)\Gamma(a)} \int_0^1 \exp(at) t^{z-t} (1-t)^{b-a-1} dt$$

The probability of detection is given by [1, 18]

$$P_d = \left(1 + \frac{2}{NR}\right)^{N-2} \left(1 + \frac{Y}{1 + \frac{NR}{2}} - 2 \frac{N-2}{NR}\right) \exp\left(-\frac{Y_b}{1 + \frac{NR}{2}}\right) \quad (5.50)$$

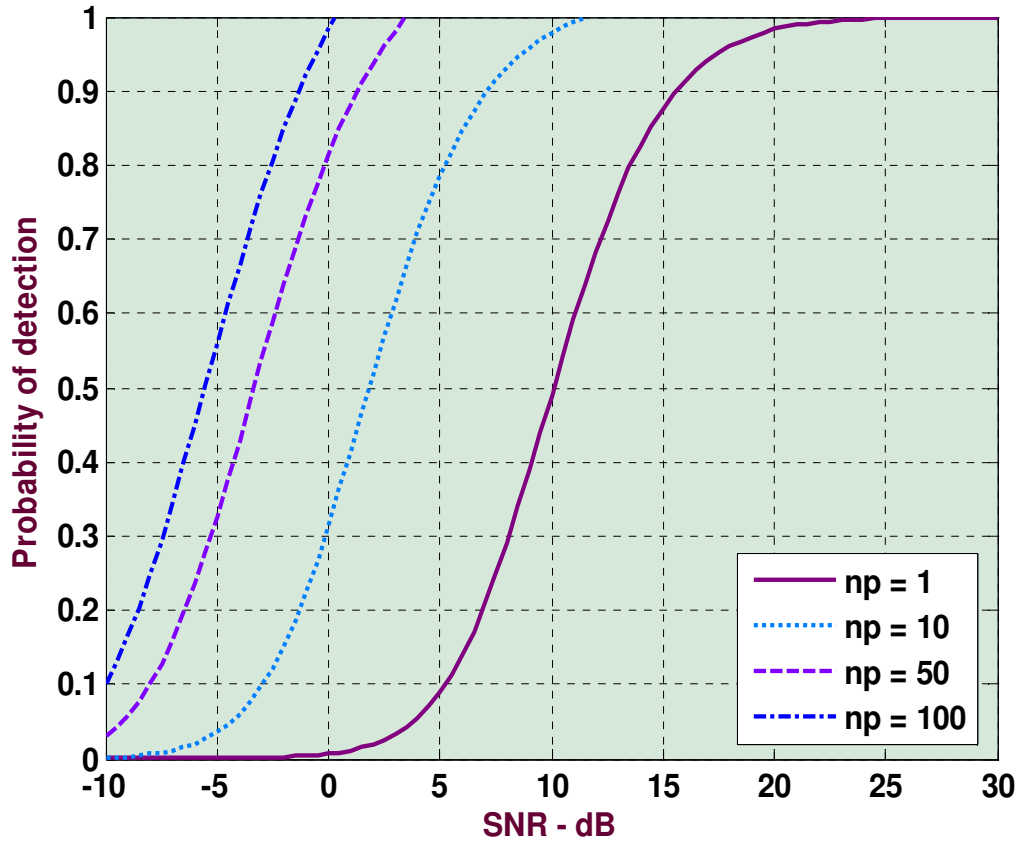


Figure 5.10 Probability of detection versus SNR. Swerling III. $P_{fa}=10^{-4}$

5.7.5 Swerling IV: fast chi-squared fluctuation

Swerling case IV is similar to case II, but the object of interest has one major reflector and many minor ones. The cross section has a chi-squared probability distribution function with four degrees of freedom and varies from echo to echo [18].

The probability distribution function for signal plus noise is given by

$$P(y) = \frac{Y^{N-1} \exp\left[-\frac{Y}{1+\frac{R}{2}}\right]}{(1+R)^{2N} (N-1)!} {}_1F_1\left(-N, N; -\frac{R}{1+R} Y\right) \quad (5.51)$$

Where ${}_1F_1$ is the confluent hypergeometric function given by

$${}_1F_1(a; b; z) = \frac{\tau(b)}{\tau(b-a)\tau(a)} \int_0^1 e^{zt} t^{a-1} (1-t)^{b-a-1} dt$$

The probability of detection is given by

$$P_d = 1 - \frac{N!}{\left(1 + \frac{2}{R}\right)^N} \sum_{k=0}^N \left(\frac{R}{2}\right)^k Y\left(N+k, 1 - \frac{Y_b}{1 + \frac{R}{2}}\right) \quad (5.52)$$

Where $Y(a, x) = \int_0^x e^{-t} t^{a-1} dt$.

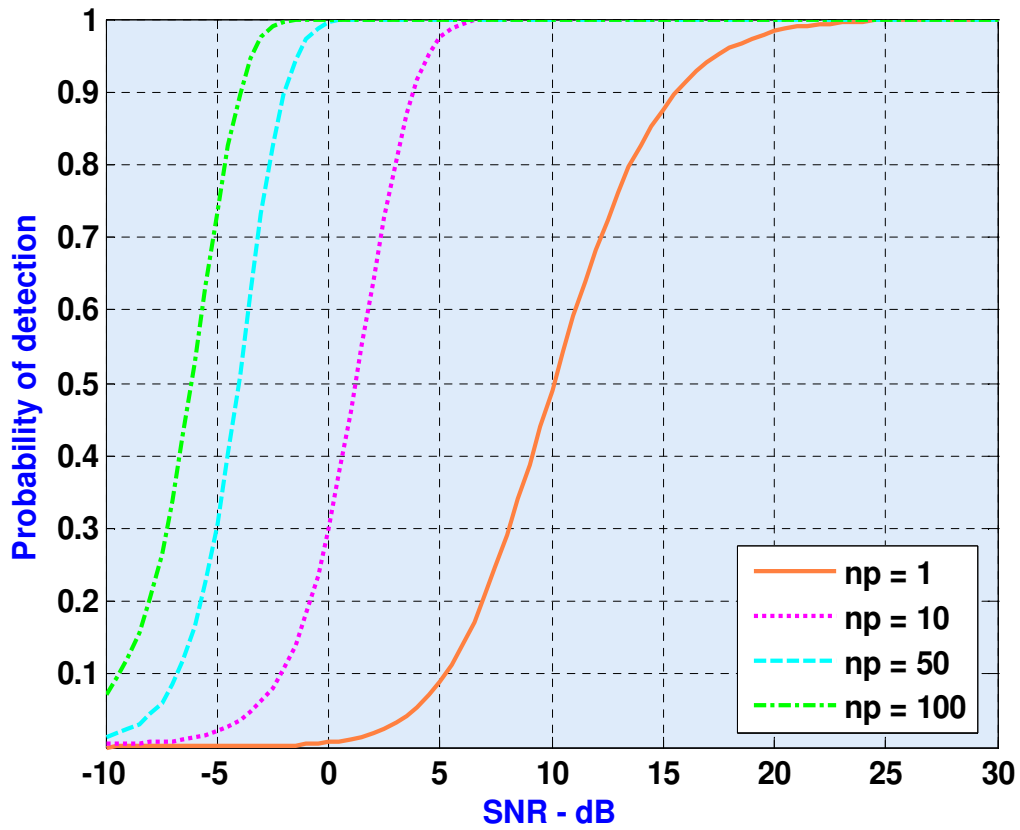


Fig 5.11 Detection of Swerling IV Targets

A comparison the four Swerling target fluctuation models and the non fluctuating case, here called case 0, is illustrated in Figure 5.6 to Figure 5.11 for n=10 hits integrated and false-alarm number of 10^4 . In general, fluctuating signals require a large signal-to- noise ratio than non fluctuating signals. The result become summarized together with fluctuation loss table 5.1

Swerling	Probability of Detection		Fluctuation loss at Pd=0.9 (dB)
	$n_p=1$	$n_p=10$	
I	0.5	0.9	10
II	0.45	0.999	10
II	0.6	0.99	4.5
IV	0.6	0.999	4.5

Table 5.1 Probability of detection for different Swerling case at SNR=12dB and fluctuation loss at Pd=0.9

Considering fluctuation loss and probability of detection Case 4 puts more demand on the jammer than do the other cases.

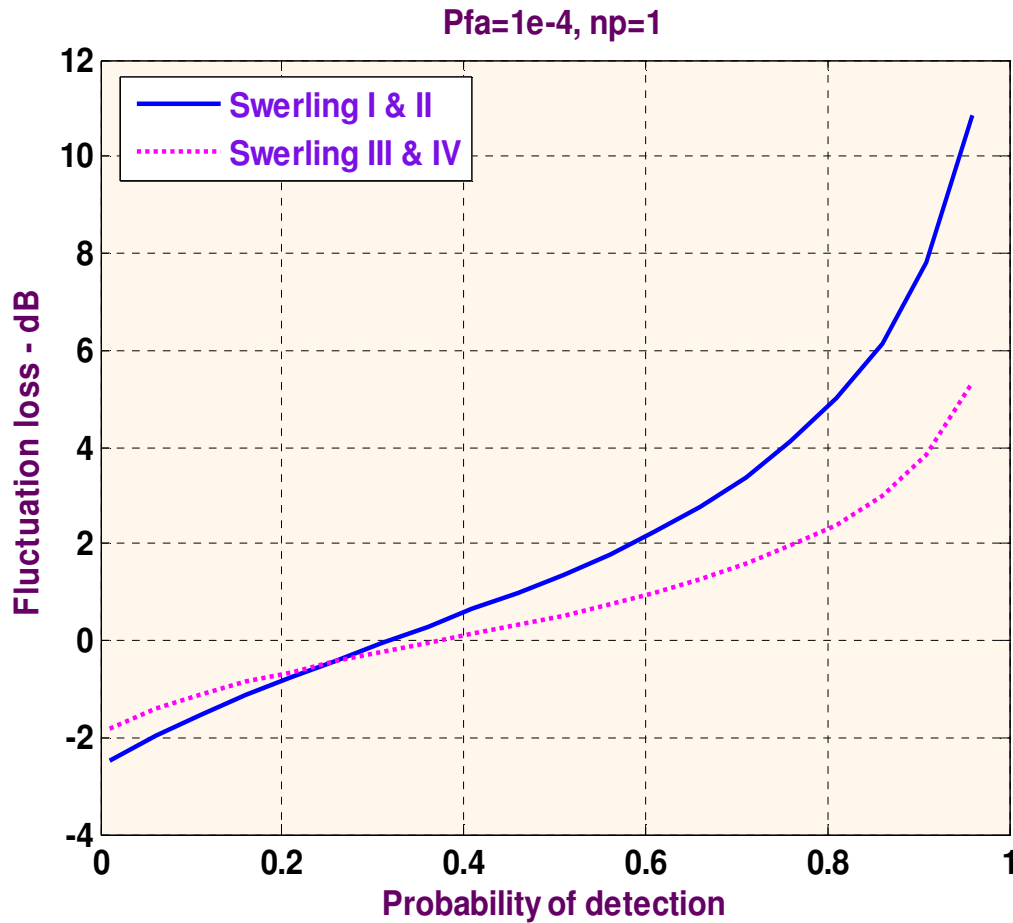


Figure 5.12 Fluctuation losses versus probability of detection

The fluctuation loss can be viewed as the amount of additional SNR required to compensate for the SNR loss due to target fluctuation, given a specific P_d value.

Note: Non-coherent integration is used for all Swerling modes, however coherent integration can be used for Swerling II and IV.

CHAPTER 6

SIMULATION AND ANALYSIS OF JAMMER

Simulation is done with the suitable types of jamming, while realized by using different mathematical expiration as derived in chapter four and five.

The jamming power is generally greater than the target signal power. In other words, the ratio S/J is less than unity. However, as the target becomes closer to the radar, there will be a certain range such that the ratio S/J is equal to unity. This range is known as the **cross-over range**. The range window where the ratio S/J is sufficiently larger than unity is denoted as the detection range. In order to compute the crossover range R_{co} , set S/J to unity in Eq. (4.21) and solve for range. It follows that

$$(R_{co})_{SSJ} = \left(\frac{P_i G \sigma B_j}{4\pi B_r L(ERP)} \right)^{1/2} \quad (6.1)$$

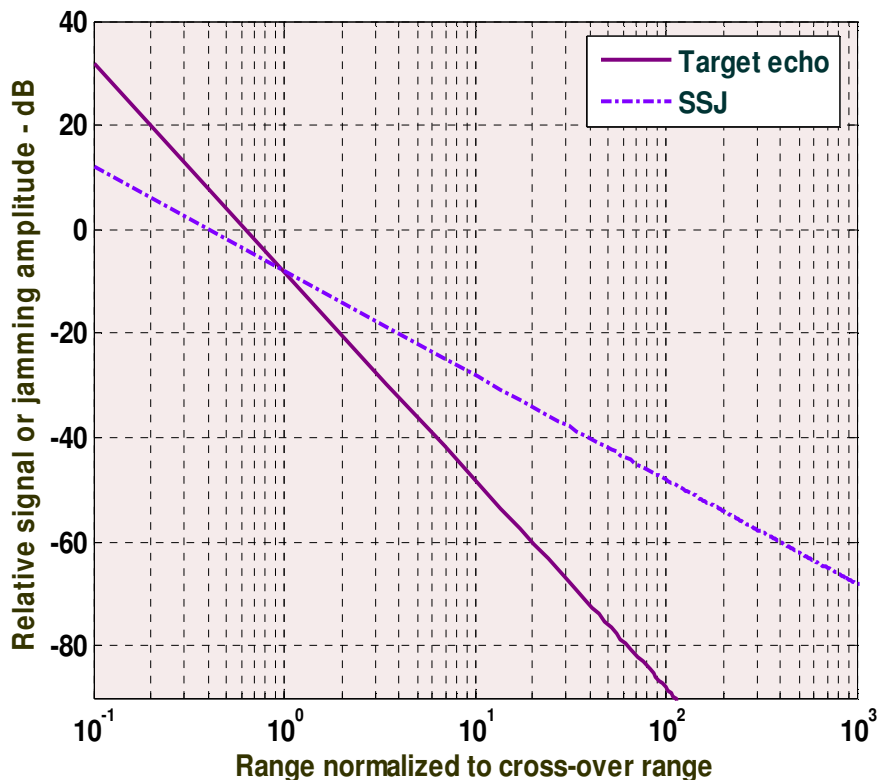


Figure 6.1 Target and jammer echo signals Figure 6.1 Plots were generated using the input parameters of P-15 radar (Appendix A) and UAV-platform jammer defined on the previous chapter, and initially assuming 50watt transmitted power. When the range less than

crossover range in this case $R = 1$ Km the echo signal can be greater than the jammer signal, and hence the jammer signal can not affect the radar operation. This implies the UAV self protected when the jammer signal greater than the echo radar signal. The effect of radar jammer peak power is shown Figure 6.2 which is inverse relation.

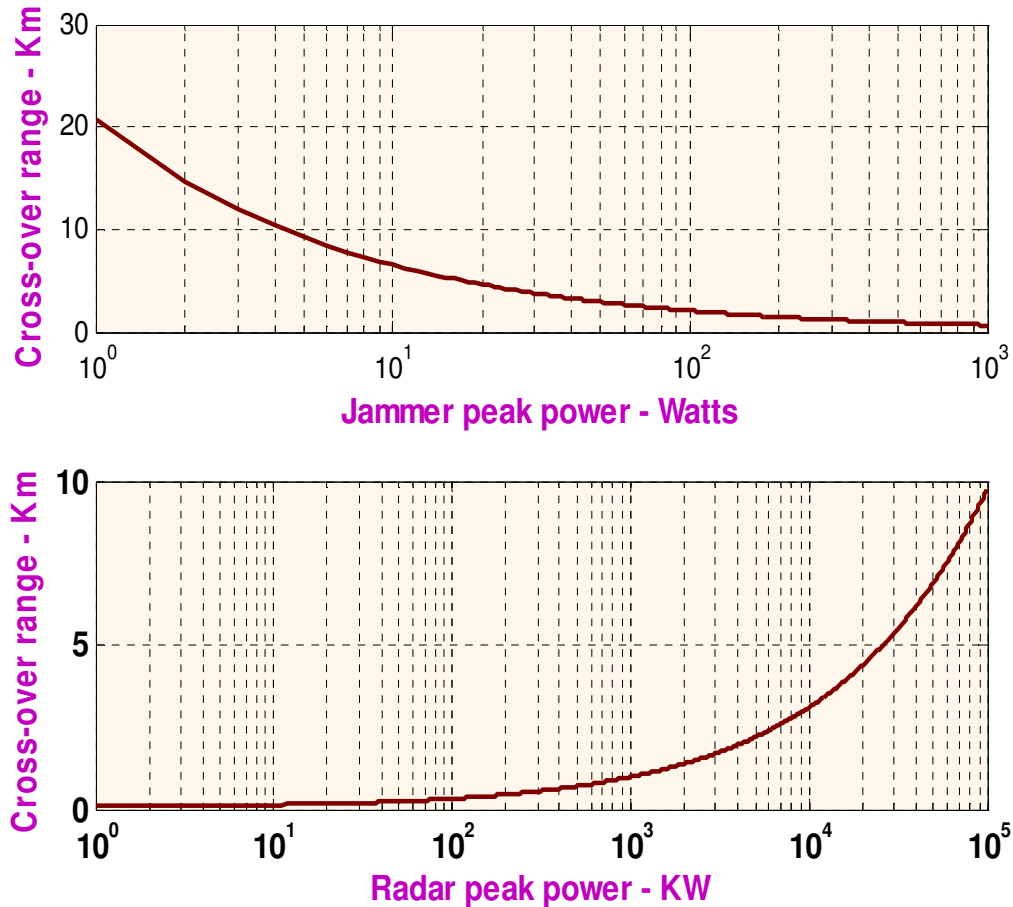


Figure 6.2 Burn-through range versus jammer and radar peak powers corresponding to example used in generating Fig. 6.1

The $S/(J+N)$ ratio should be used in place of the SNR when calculating the radar equation and when computing the probability of detection. Furthermore, $S/(J+N)$ must also be used in place of the SNR when using coherent or non-coherent pulse integration.

The range at which the victim radar can detect the screened target, called the **burn-through range** [25] is given $S/(J+N)$ value is defined as the burn-through range.

It is given by, which is derived from Eq. (4.22) [24, 8].

$$R_{BT} = \left\{ \left(\frac{(ERP)A_r}{B\pi b_j K T_o} \right)^2 + \frac{P_i G 6 A_r \tau}{(4\pi)^2 L \frac{s}{(J+N)} K_{T_o}} - \frac{(ERP)A_r}{8\pi B_j K T_o} \right\}^{1/2} \quad (6.2)$$

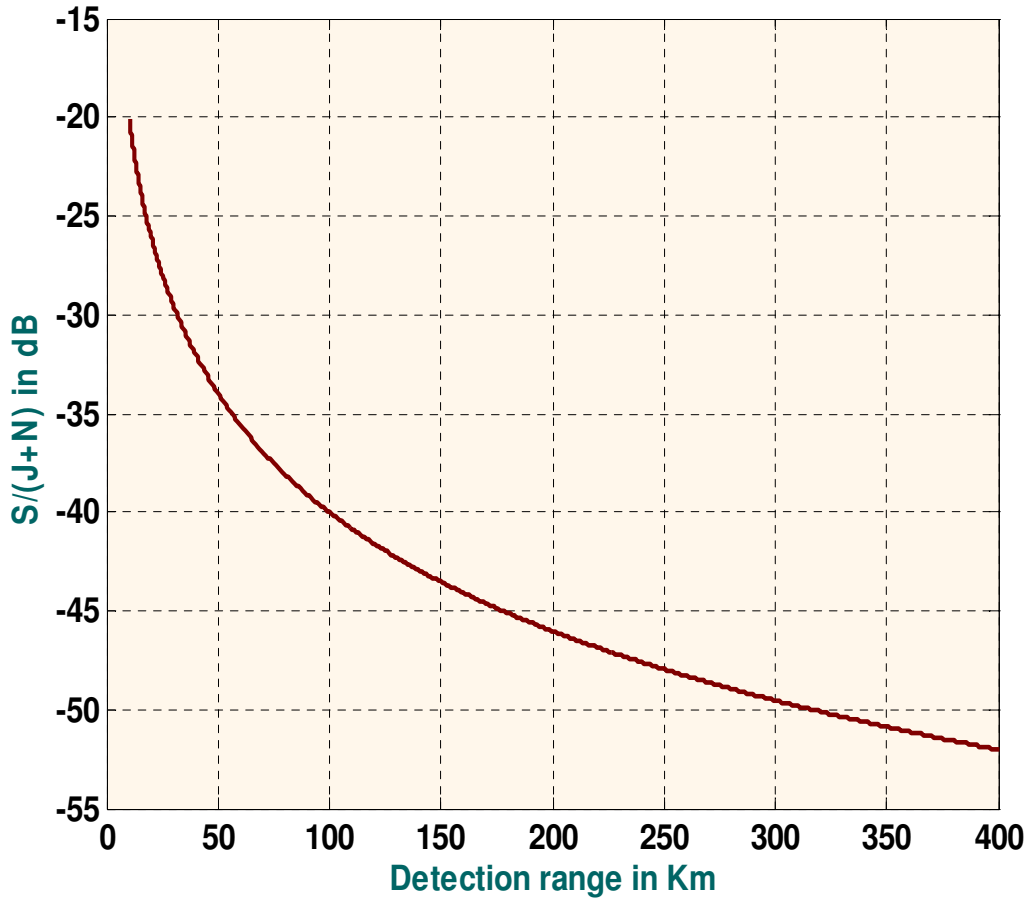


Figure 6.3 $S/(J+N)$ versus detection range

Figure 6.3 shows the effect of jamming and noise signal to the radar detection range. Assume the UAV can near to the radar about 50km (the range of missal attack) and can be used as stand in jammer in this case the $S/(J+N)=-34\text{dB}$ this data can be used an input parameter for Figure 6.4 which provides jammer ERP equal to 6 dB .Using the equation (4.14) and Figure 6.4 the jammer transmitted power for stand in jammer become 6.3 watt.

Fig 6.4 shows the range for the radar in this thesis $S/(N+J) =-34\text{dB}$, for a 1m^2 target as a function of jammer ERP. Smaller targets will not produce the required $S/(J+N)$ with the optimum pulse durations.

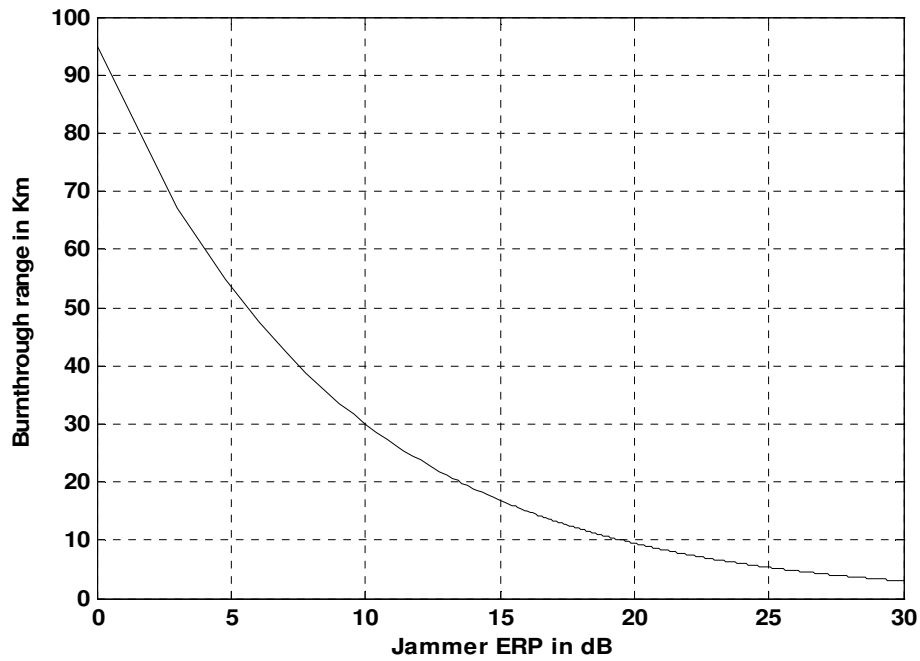


Figure 6.4 Burn-through ranges versus ERP. ($S/(J+N) = -34$ dB)

Using the general equation Eq.(4.29)the jammer signal versus normalized range can be plot

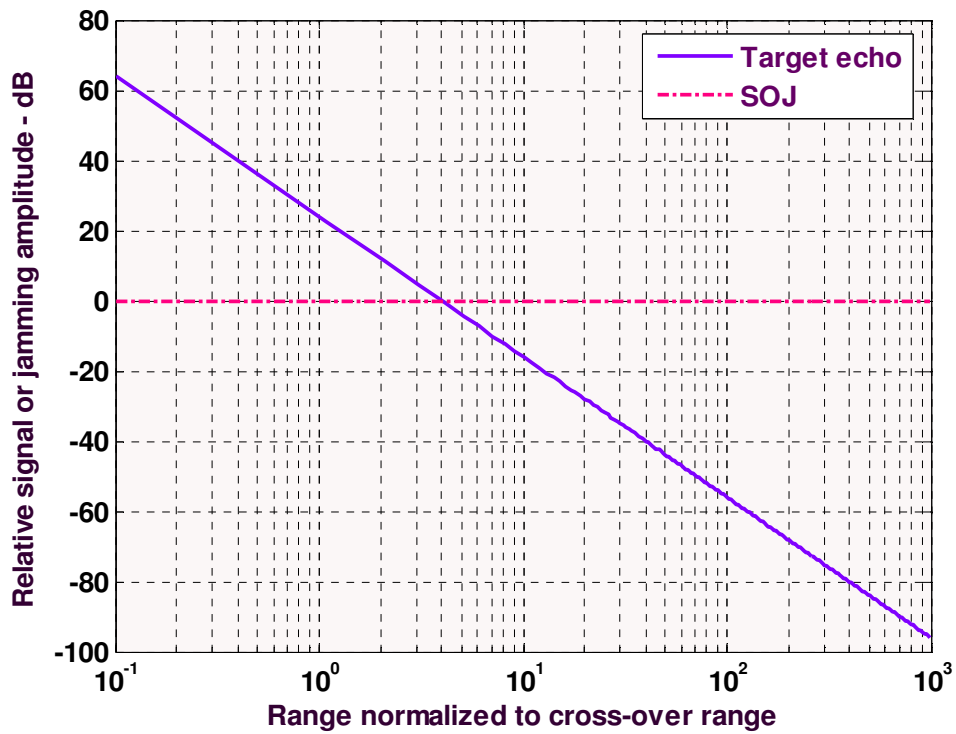


Figure 6.5 Normalized range versus Jammer amplitude for SOJ

To present the values of J and S, (or J/S) over a minimum to maximum radar to target range of interest, this has a slope of 4 dB for J vs. range as shown Figure 6.5

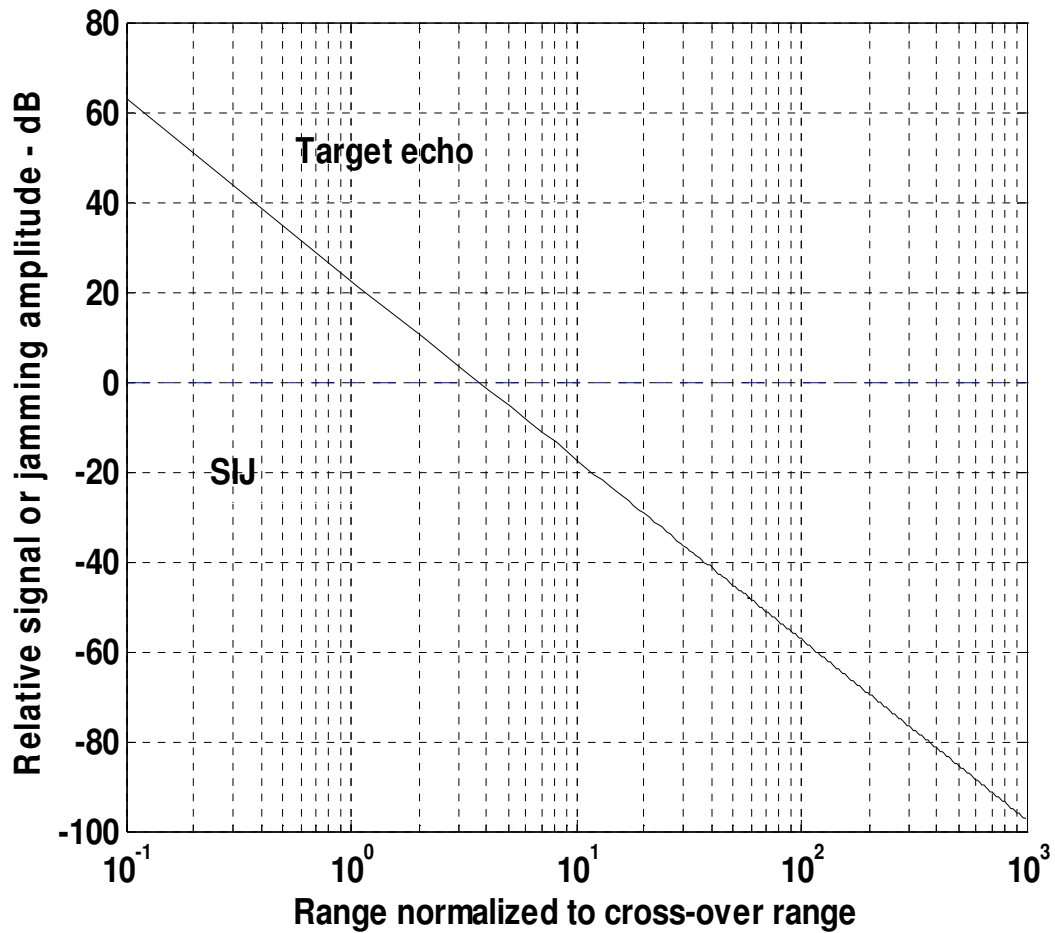


Figure 6.6 Range versus Jammer amplitude for SIJ

The cross over range is slightly less than stand of jammer, as shown in the Figure 6.6. However the jammer need less power as compare with stand off jamming i.e. it need **6.3 watt**, actually the return signal power can be very small compare with stand in jamming, usually in microwatt.

The command and control device can be decide the jammer type after this result i.e. when the required jammer transmuted power is 6.3 watt ($R < 50$ Km) stand-in jamming, when the transmitted power 50 watt ($\text{Range} > 50$ Km) stand-off jamming. The logic is simple (for instance: 00=No jamming, 01 self-screen jamming, 10 stand off jamming, 11 stand in jamming).

The amount of reduction in the signal-to-noise plus interference ratio because of the jammer effect can be computed from the difference between Eqs. (4.39) and (4.43). It is expressed (in dB) by

$$\gamma = 10 \log \left(1 + \frac{T_f}{T_e} \right) \quad (6.3)$$

Consequently, the PRF is

$$PRF = 10^{\frac{-\gamma}{40}} \quad (6.4)$$

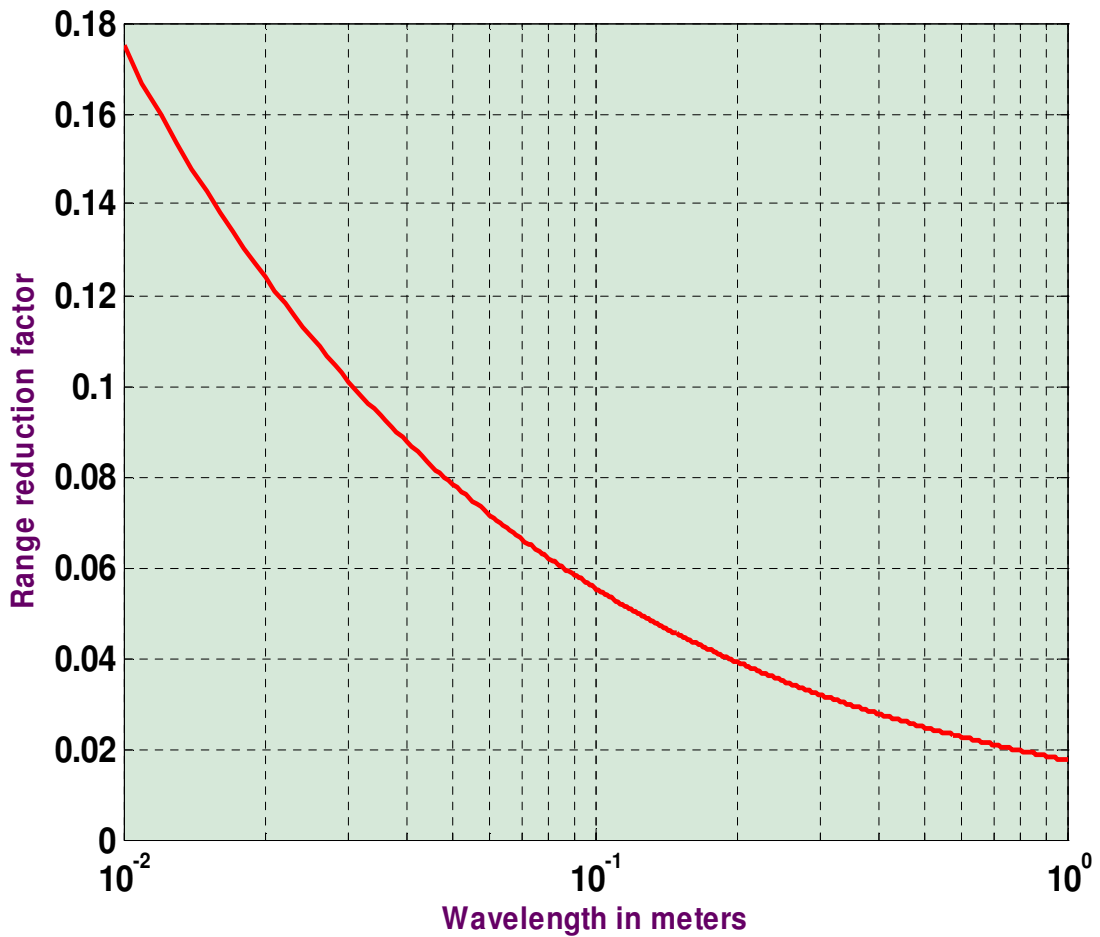


Figure 6.7 Range reduction factor versus radar operating wavelength

Since the radar operating frequency equal to 750MHz, which implies the wavelength of the radar become 0.4 m and hence the range reduction factor become 0.029, see Fig.6.7

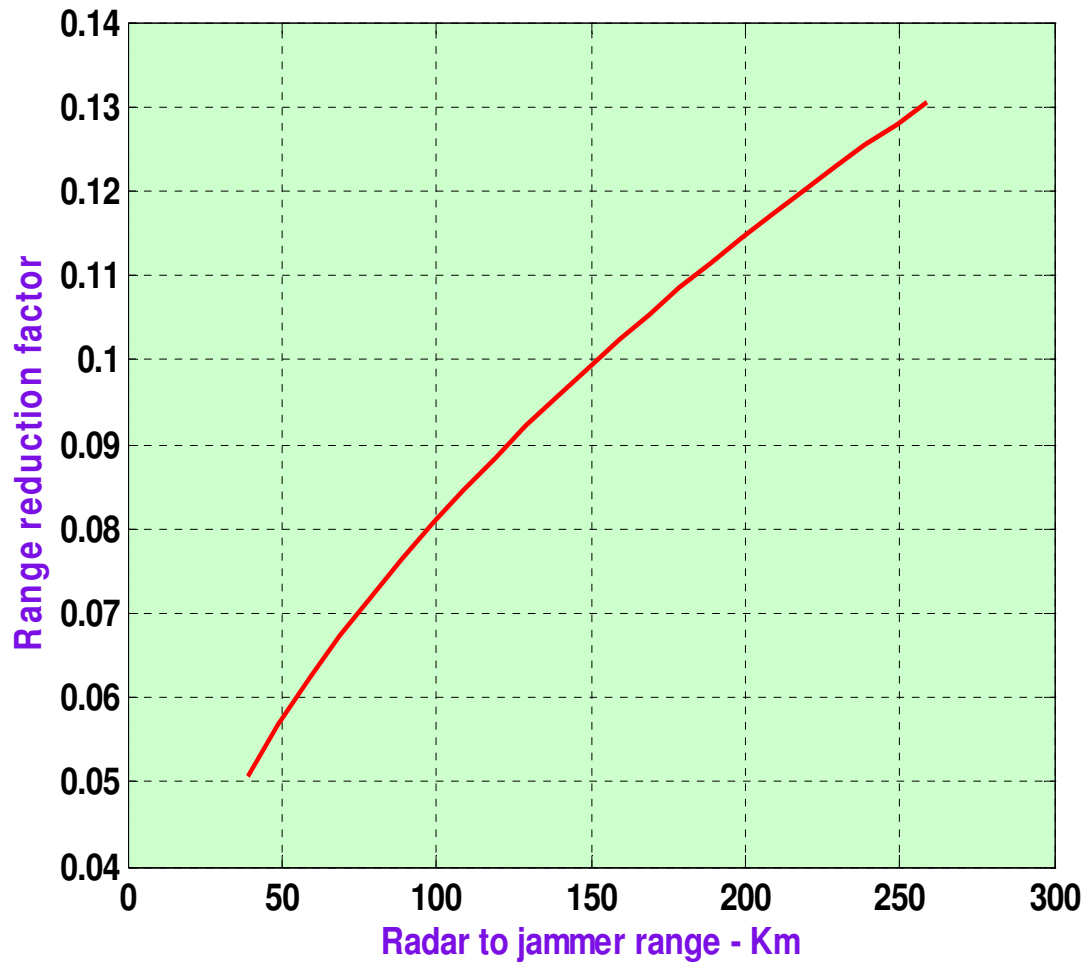


Figure 6.8 Range reduction factor versus radar to jammer range

The same effect as above case except slightly difference, at 130 Km the range reduction factor become approximately 0.028. For stand in jamming at 50 Km the range reduction factor approximately 0.017 which is shown Fig. 6.8

The second type of jamming techniques is repeater jamming, the effect of this type of jamming can be seen Figure 6.9, by using equation (4.38), i.e.

$$P_J = \frac{P_T G_T L_p \sigma_e}{4\pi R^2 G_{JT} \beta^2}$$

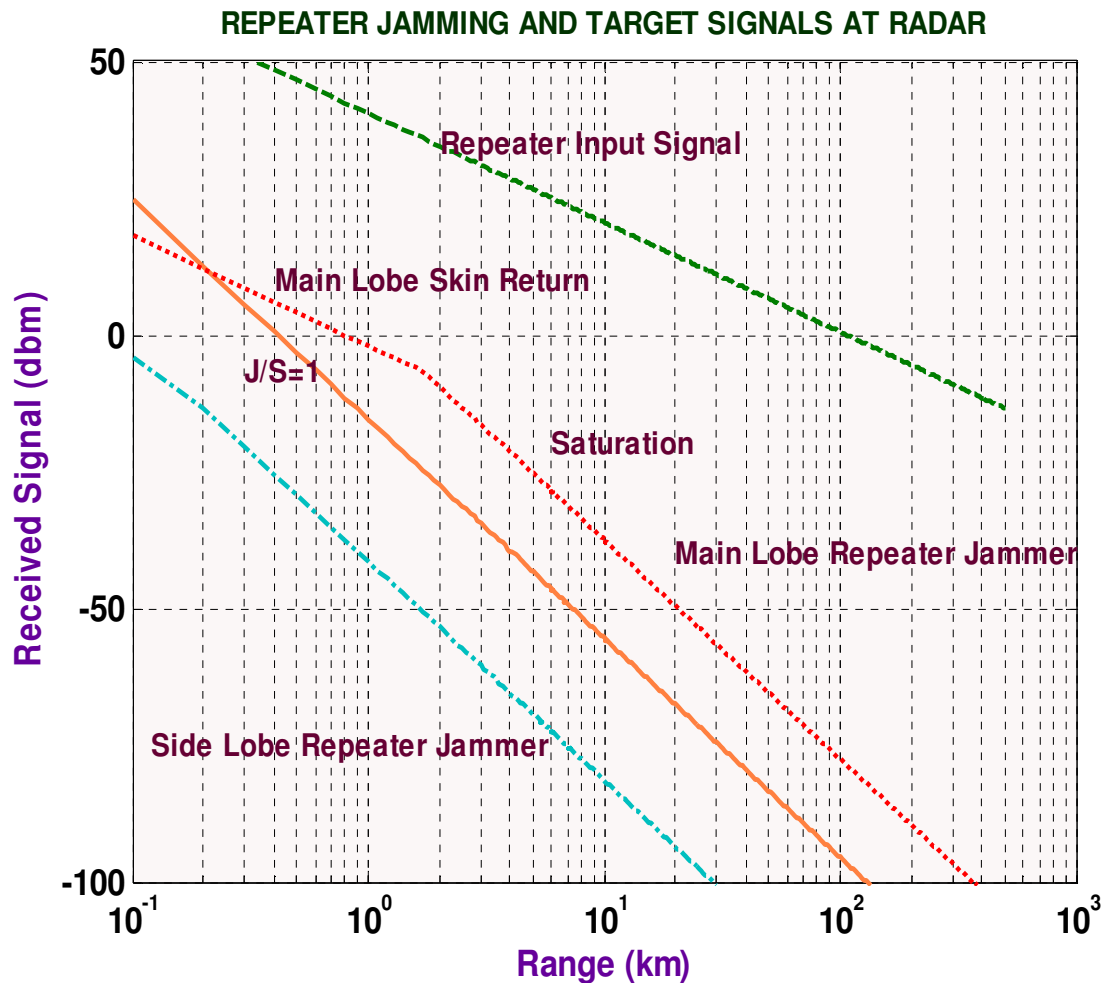


Figure 6.9 Repeater jamming

The crossing of the J and S lines (known as crossover) gives the range where $J = S$ (about 0.3 Km), and shows Fig.6 9 that shorter ranges will produce target signals greater than the jamming signal.

As chapter four describes a point where the radar power overcomes the jamming signal is known as **burn-through**. The crossover point where $J = S$ could be the burn-through range, but it usually isn't because normally $J/S > 0$ dB to be effective due to the task of differentiating the signal from the jamming noise floor.

Radar can be designed with higher power than the necessary power for earlier burn-through on jamming targets. Naturally that would also have the added advantage of earlier detection of non-jamming targets as well. Since the jammer on the target amplifies the received radar signal before transmitting it back to the radar, both J and S experience the two way range loss.

Normally, the constant gain (linear) region of a repeater jammer occurs only at large distances from the radar and the constant power (saturated) region is reached rapidly as the target approaches the radar.

Once the jammer output reaches maximum power, that power is constant and the jamming slope changes since it is only a function of one way space loss and the J/S the cross over range is less than 0.2 Km, which is better than noise jamming, however implementation of repeater jammer is difficult for UAV-platform jammer.

Now consider the effect of Swerling case for jamming. The simulation result found in Fig.6.10 and Fig 6.11 using Equation (4.44 to 4.50); a bar chart of the detection ranges with and without jamming for the five Swerling types are illustrated from thus figure.

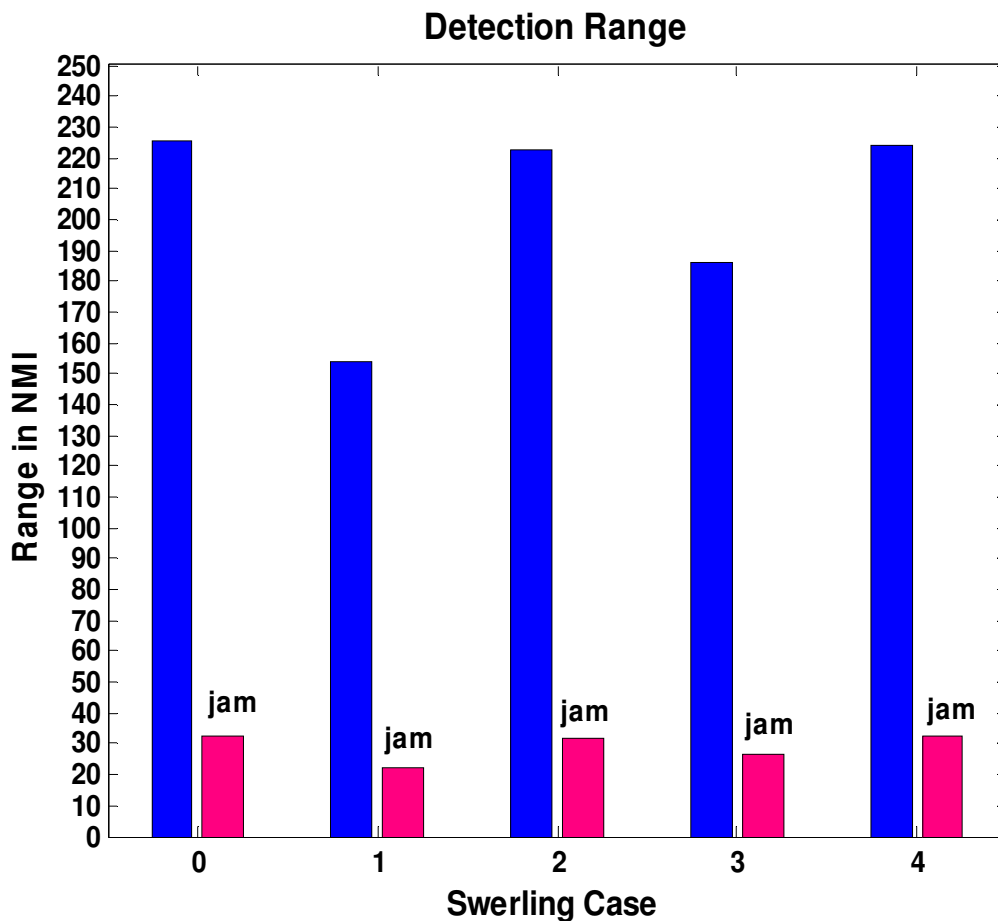


Figure 6.10 Stand-off jamming effect using Swerling case

Figure help to determine the detection range of the P-15 radar for 1m^2 target in the clear and in the presence of stand-off jammer, positioned at 130 Km (26,000-ft altitude which the maximum height of Predator-UAV). The length of the target is equal to 8.2 m (UAV length) at Ethiopia (North) under worst case of atmospheric temperature, i.e. 318^0 K .

From fig. 6.10 it is clear that the jammer effect of Swerling 0, II, and IV cases are almost the same , However by considering the fluctuation loss, from Table 5.1, the jammer performance have been good enough for Swerling 4 case, thus it can be implemented.

The same analysis can be taken for stand-in jamming as shown in Figure 6.11, but the jammer power and range are lesser than that of stand-off jamming. The over all effect is that about 93 % range reduction can be achieved from Swerling case IV.

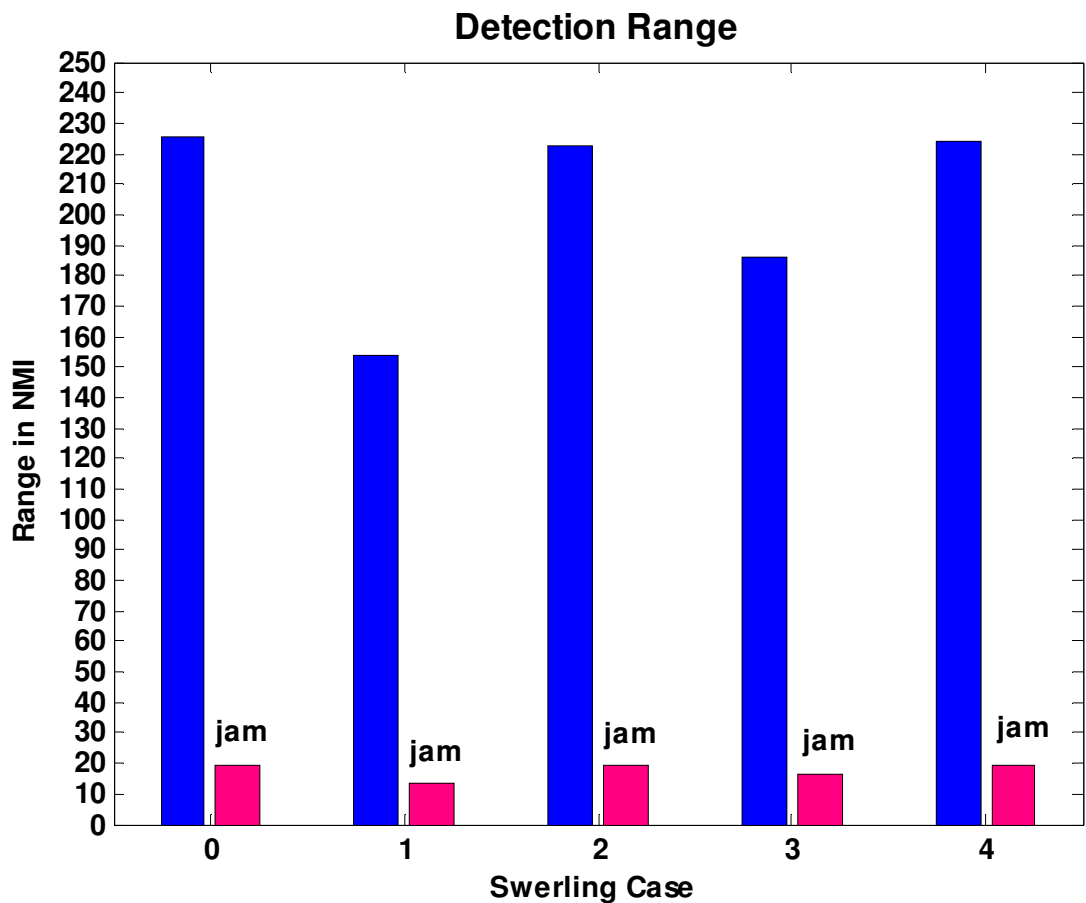
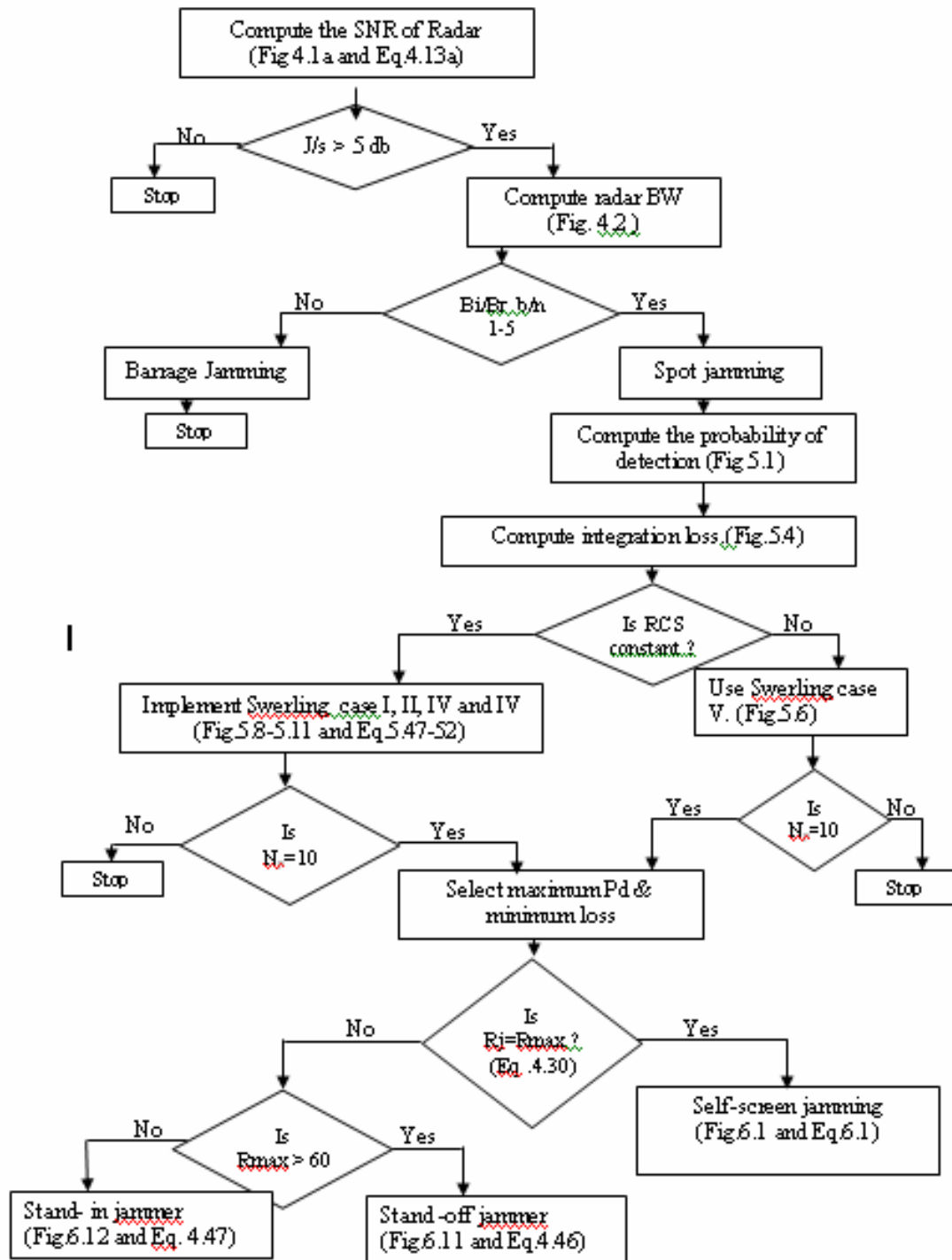


Figure 6.11 Stand-in jamming effect using Swerling case

The jammer flow chart for the simulation is helpful to summarize the analysis and it is given below. The concerned mathematical expressions and figure are mentioned in the jammer flow chart



CHAPTER 7

CONCLUSION AND FUTURE WORK

Successfully denying the use of the radar spectrum is the purpose of Electronic attack EW. It depends on many factors, including the distance between the radar and the jammer, the ERP from the jammer relative to the ERP of the radar transmitter and receiver.

Because the Predator is unmanned it is suitable for deployment in "moderate risk areas", i.e., unsecured air space. The Predator system was designed to provide constant intelligence, surveillance, reconnaissance for strategic and tactical forces. In this thesis UAV is used for radar jamming purposes.

In this thesis interception of P-15 radars' signal by the jammer-receivers have been described. The jammer receiver allows the threat to be identified and the parameters set to be updated with the latest information relevant to the specific emitter which is to be jammed (such as frequency, pulse width). The command and control system of the jammer can be decided by using this parameter (jam or no jam). The jammer waveform is then synthesized at DDS and used to generate multiple synchronized random jamming pulses that are received through the radar antenna.

Stand-in jamming is more effective than stand off jamming for UAV-Platform by decreasing the jammer transmitted power and by attacking the radar main lobe. In addition to this the jammer performance can be increased by using pulse integration technique, in this case the pulse integration loss must be taken into consideration (i.e. if the number of pulse-integration is increased then the integration loss also increases). For fluctuation signals Swerling IV case is more preferable for this particular jamming platform.

For stand-in (at 50Km) $P_t = 6.3$ watt, antenna gain = 12 dB, $P_d = 0.9$, $B_j = 2$ MHz, jammer loss of 14dB and jammer EIRP = 15dB with UAV-altitude of 7 Km and under worst environment condition of Ethiopia (temperature=318 K and rainfall up to 10mm/hr) is sufficient to provide jamming for P-15 radar signal.

Deploying Radar jammers on UAV has several advantages. The first of these is fratricide avoidance. Standoff jammers, being closer to friendly radar or radios than the targets, can inject unwanted, interfering energy into the friendly radar/communication systems. By placing the jammer in the adversary's battle space, normally all radars placed there can be viewed as targets so the fratricide problem disappears.

A second advantage of UAV jammers is their minimal vulnerability as one of the problems with manned jammer is their survivability once they are put into operation. Such high-power transmitters are relatively easy to find both in frequency and geo-location. This makes them particularly vulnerable to enemy attack, from direct fire as well as indirect fire weapons, either of which could involve homing weaponry.

The application of this jamming is to protect our country from enemy attack with endangering human pilot's life. In Ethiopia geographical nature, UAV-borne jammer is substantially less vulnerable and more survivable. In addition to this economical viability is also worth to consider.

Future work

This study could cover some of the advantages; however it has also some limitation. Now a days more advanced techniques are employed in modern radar, these include pulse compression, pulse Doppler, and ultra low side lobe antenna. All these techniques make difficult to jam the modern radars. Thus there is a need for further studies on special EA techniques for effective jamming such as **half code repeater jammer**.

References

- [1] Michael O.Kolewole, PhD, “*Radar systems, peak Detection and Tracking*” Amsterdam, Liuaire, Houle, Jordan Hill, 2002, P: 64, 66,107-108,111-120,126-132,279,281.
- [2] Merrill I. Skolnik, “*Introduction to Radar system*”, second ed. United State, Mc Graw-Hill, Inc, 980. P: 7, 19, 23, 47-56,152,226,227,460.
- [3] Richard A.Poisel, “*Introduction to Communication electronic warfare system*”, Boston. London, Artech House, 2002, P: 189,449,509.
- [4] Richard I. Wiegand, “*Radar Electronic Countermeasures System Design*”, London, Artech House, Inc, 1991, P: 11, 18, 47, 183.
- [5] Rowun Gilmore, “*Practical RF circuit Design for Modern Wireless System*”, Volume 1, Boston, Artech House, Inc 2003 P: 81-85.
- [6] Bernard Sklar, “*Digital Communication Fundamental and Applications*”, Second Edition, New Jersey, P: 169,171,178,251,253,254.
- [7] W.Alan Davis, Krisha Agarway,” *Radio frequency Circuit Design*”, New York/Tronto, John Wily and sons, inc. 2001, P: 121,168,222.
- [8] David L. Adamy, “*Introduction to Electronic warfare modeling and simulation*”, Canton Street, Artch House, 2003, P: 9,10,14,16.
- [9] Mugu, “*Electronic warfare and Radar systems Engineering Handbook*”, Washington D.C, April 1999, section 4-4.5, 4-7.5, 4-.1, 4-10.1.
- [10] James D.Taylor,”*Ultra-wideband Radar technology*,” Florida, CRC Press, 2000, P: 133.
- [11] Lalchand Godara, “*Hand book of Antennas in wireless Communication*”, New York, CRC Press LLC, 2002, P: 142- 183.
- [12] Sophocles J.Orfandis,” *Electromagnetic Waves and Antennas*,” Rutgers University, June 21, 2004, P: 489-493, 529.

-
- [13] Philippe Lacomme, Jean, Clavde Marchualos, “*Air and Space borne Radar system: An Introduction*”, United state of America William Andrew publishing, LLC, 2001, P: 22-60, 133-145, 350-385.
- [14] D.curtis Schleher, “*Electronic warfare in the information Age*,” Boston. London, Artech House, 1999, P: 13-20, 65, 67, 147-157.
- [15] Pokka Eskellnen, “*Introduction to RF equipment and system Design*”, London, Artech house, Inc, 2004, P: 42-48.
- [16] Devendra K. Misra, “*Radio-Frequency and microwave communication Circuit Analysis and Design*”, Singapore, Jon Wiley and Sons, inc. 2001, P: 513.
- [17] Vinary ki.Ingle John G.Proakis, “*Digital signal processing using matlab V.4*”, New York, PWS Publishing Company, 1997.
- [18] Hamish, “*Modern Radar*”, London, Artech House, Inc, 2001,P: 161,169.241- 248.
- [19] Peyton Z.Peebles, Jr., ph.D “*Probability, Random Variables and random Signal Principles*”, Second Edition, New York, McGraw-Hill, inc, 1987, P: 43,105.
- [20] Hweip. Hsu. PhD, “*Theory and Problems of Probability, Random variables, and Random Processes*”, New Jersey; Mc Graw Hill, 1996, P: 213.
- [21] Saeed V. Vaseghi, “*Advanced Digital Signal Processing and Noise reduction*”, third Ed, UK, John Wilen & Sons, Ltd, 2006, P: 5, 23-26.
- [22] George W.Stimson,” *Airborne Radar*”, Second Edition, New Jersey, Scitech publishing, inc., 1998, P: 83-135, 439-469.
- [23] Harlod R.Raemer,”*Radar System Principles*,” London, CRC Press LLC, 1997, P. 35-41, 87-156,425-433.
- [24] G. Richard **Curry**,” *Radar System Performance Modelling*”, Second Edition, Artch House, London, 2005, P: 63-67,87-100.
- [25] David K. Barton, Sergey A.Leono,”*Radar Technology Encyclopedia*,” London, Artech House, 1997, P: 169-171,206,233-240,269-271,448
- [26] Mourad Barkal,”*Signal Detection and Estimation*”, Second edition, Boston/London, Artech House, 2005, P: 99-105, 348.
- [27] Mike Golio, “*Microwave and RF product Application*”, New York, Washington, D.C., CRC Press, 2000, P: 13-1, 14-1, 14-2.
- [28] Victory C. Chem., “*Time-Frequency Transforms for Radar imaging and Signal*

-
- Analysis”, London, Artch House, 2000, P: 17.
- [29] Richard C. Dorf, “Electronic, Power Electronic, Microwave, Electromagnetic, and Radar”, Third edition, U.S.A, CRC, 2005, P: 20-29.
- [30] Gospare Galati, “Advanced Radar Techniques and Systems”, United Kingdom, Peter Peregrinus Ltd, 1993, P: 145-150,565.
- [31] Merrill Skolnik, “Radar Handbook”, Second Edition, New York, Mcc Graw Hill, 1990,P: 2-26,3-32.
- [32] Fred E. Nathanson , “Radar Design Principles, signal processing and the Environment”, Second edition, New Jersey, INC, 1999, P: 63-64.87.
- [33] http://www.ethiomet.gov.et/pdf_files/Belgseasonalclimate2006.pdf
- [34] <http://www.globalsecurity.org/military/world/russia/flat-face.htm>
- [35] <http://www.elsys.com.ua/radars/land-radar-p-15.html>
- [36] IEEE Standard, *Test procedures for Antenna*, New York, the institute of electrical and electronics Engineers, Inc, December 15, 1977, P: 18, 142.

APPENDIX A

P-15 Radar Specification

(The parameters are not found with in a single source some of them are [34.35])

Operating Frequency	750MHz
Pulse Repetition frequency (PRF)	500 to 600 pulse/sec
Pulse Repetition Time (PRT)	2 to 4 millisecond
Peak Power	300 to 900 Kw
Effective Range	210 to 250km
Accuracy	5 ⁰ (angular), 90m(R)
Pulse-Width	2 to 3 microsecond
Beam width	2 ⁰ horizontal, 5 ⁰ Vertical
Antenna gain	26 to 32 dB
Noise Figure	3dB
Polarization	horizontal
Antenna	parabolic
Limitation	wind (Km/h) 90

APPENDEIX B

MATLAB CODE

```

% this program implements Eq. (4.13a)
%-----

Pt = 10*log10 (Pt); % convert peak power to dB
wl_sqdb = 10*log10 (WL^2); % compute wavelength square in dB
c = 3.0e+8; % speed of light
wl = c / fr; % wavelength
rcsdb = 10*log10(rcs); % convert rcs to dB
Four_Pi_Cub = 10*log10 ((4.0 * pi) ^3); % (4pi) ^3 in dB
k_dB= 10*log10(1.38e-23); % Boltzman's constant in dB
te_dB= 10*log10(te); % noise temp. in dB
b_dB= 10*log10(b); % bandwidth in dB
R_pwr4_dB= 10*log10 ((R). ^4); % vector of target R^4 in dB
nominator = Pt + G + G + wl_sqdB+ rcsdb;
denominator = Four_Pi_Cub + k_dB+ te_dB+ b_dB+ nf + L + R_pwr4_db;
snr = nominator - denominator;
return
function [BR_R] = standoff_jammer (Pt, g, rcs, b, fr, L, R, ...
    pj, bj,gj, Lj, gprime, Rj)

% this function use for burn through range

function [R] = burn_jammer (Pt, g, rcs, fr, tau, T0, L, pj, bj, gj, Lj,sir0,ERP);
%-----
k = 1.38e-23;
%R = linspace(rmin, rmax, 1000);
c = 3.0e+8;
sir0 = 10^(sir0/10);
wl = c / fr;
gj = 10^(gj/10);

```

```

G = 10^(g/10);
Ar = wl *wl * G / 4 /pi;
nominator32 = ERP .* Ar;
demo3 = 8 *pi * bj * k * T0;
demo4 = 4^2 * pi^2 * k * T0 * sir0;
val1 = (nominator32 ./ demo3).^2;
val2 = (Pt * tau * G * rcs * Ar)/(4^2 * pi^2 * L * sir0 * k *T0);
val3 = sqrt(val1 + val2);
val4 = (ERP .* Ar) ./ demo3;
R = sqrt(val3 - val4) ./ 1000;
figure (1)
plot (10*log10(ERP), R, 'k')
xlabel ('Jammer ERP in dB')
ylabel ('Burn through range in Km')
grid
% this matlab code produces Fig 6.2
%-----
clear all
Pt = 900.0e+3;
G = 32.0;
fr = 7.5e+8;
rcs = 1.0 ; % radar cross section( m2)
B= 500.0e+3; % radar operating bandwidth ( Hz)
L = 8; % radar losses (dB)
Rj = 120.0; % range to jammer (Km)
pj = 50.0; % jammer peak power (Watts)
bj = 2.0e+6; % jammer operating bandwidth ( Hz)
gj = 12.0; % jammer antenna gain ( dB)
Lj = 14; % jammer losses (dB)
[BR_R] = selfscreen_jammer (Pt, g, fr, rcs, b, L, ...
pj, bj, gj, Lj)

```

```

% this matlab code produce Fig 6.6
%-----
clear all
Pt = 900.0e+3;
G = 32.0;
fr = 7.5e+8;
rcs = 1 ;
B= 500.0e+3;
R = 130;
gprime = 12.0;
L = 8;
Rj = 120;
pj = 50;
bj = 2e+6;
gj = 12.0;
Lj = 14;
standoff_jammer (Pt, G, rcs, b, fr, L, R, ...
    pj, bj,gj, Lj, gprime, Rj)
grid
% Fig 6.9
%-----
% Clear Old Variables
clear,clc,clf;
Rmin=.1; Rmax=500;    % km
% Define Rtar(km) from Rmin to Rmax
Rtar=Rmin:.1:Rmax;    % .1 km steps
% Radar and Target Parameters
Pt=9e5;              %
Gt=10^(32/10);
Gr=10^(32/10);
rcs=1;              % sq m

```

```

wl=0.4;          % m
Lr=10^(8/10);
Gsl=10^(10/10) % dbi (Near-In Sidelobes)
% Calculate Target Power Received at Radar
Pr=(Pt*Gr^2*rsc*wl^2)/((4*pi)^3*Lr*(Rtar*10^3).^4);
Prdbm=30+10*log10(Pr);
% Jammer Related Parameters Pjsat=50;          % w
Gjr=10^(12/10);
Gjt=10^(12/10);
Lp=10^(3/10);          % Loss 1
Beta=1;          % Loss 2
Lj=10^(11/10);          %Loss 3
effrcs=10*rsc;          % Effective RCS
% Calculate Power Received by Jammer
Pjr=Pt*Gt*wl^2*Gjr./((4*pi*Rtar*10^3).^2*Lp);
Pjrdbm=30+10*log10(Pjr);
% Calculate Repeater Gain
Grep=4*pi*effrcs*(Lp^2)/((wl^2)*Beta^2);
% Calculate Repeaters Electronic Gain
Ge=Grep/(Gjr*Gjt);
% Calculate Jammer Power
Pj=Pjr*Ge;
for i=1:length(Rtar);
    if Pj(i)>Pjsat;Pj(i)=Pjsat;end;
end;
% Calculate Jam Power at Radar Receiver
Prj=Pj*Gjt*Gr*wl^2./((4*pi*Rtar*10^3).^2*Lp);
Prjdbm=30+10*log10(Prj);
% Calculate Sidelobe Jam Power at Radar
Pjrsl=Pjr*Gsl/Gt;
Pjssl=Pjrsl*Ge;
for i=1:length(Rtar);

```

```

    if Pjisl(i)>Pjsat;Pjisl(i)=Pjsat;end;
end;
Prjisl=Pjisl*Gjt*Gsl*w1^2./((4*pi*Rtar*10^3).^2*Lp);
Prjslldbm=30+10*log10(Prjisl);
% Plotting Received Target and Jammer Signals
semilogx(Rtar,Prdbm,Rtar,Pjrdbm,Rtar,Prjdbm,Rtar,Prjslldbm);
ylabel('Received Signal (dbm)');
xlabel('R (km)');grid;
title('REPEATER JAMMING AND TARGET SIGNALS AT RADAR');
axis([.1,1000,-100,50]);
text(2,35,'Repeater Input Signal');
text(20,-40,'Main Lobe Repeater Jammer'); text(.12,-75,'Side Lobe Repeater
Jammer');
text(.4,10,'Main Lobe Skin Return');
text(6,-20,'Saturation');
text(.3,-7,'J/S=1');
%ssj_reqi
clear all
Pt = 900.0e+3;
G = 32.0;
fr = 7.5e+8;
rcs = 1.0 ;
B= 500.0e+3;
L = 8;
Rj = 120.0;
pj = 50.0; % jammer peak power in Watts
bj = 2.0e+6; % jammer operating bandwidth in Hz
gj = 12.0; % jammer antenna gain in dB
Lj = 14; % jammer Les in dB
[BR_R] = ssj_req (Pt, g, fr, rcs, b, L, ...
pj, bj, gj, Lj)

```

Note: This matlab code shows only sample of the study

